The Belledonne border fault: identification of an active seimic strike-slip fault in the western Alps

François Thouvenot, Julien Fréchet, Liliane Jenatton, J.F. Gamond

Geophys. J. Int. (2003) **155,** 174–192

The Belledonne Border Fault: identification of an active seismic strike-slip fault in the western Alps

François Thouvenot,[1] Julien Fréchet,[1,2] Liliane Jenatton[1] and Jean-François Gamond[1]

[1]*Laboratoire de Géophysique Interne et Tectonophysique (CNRS/UJF), Maison des Géosciences,* BP 53, 38041 *Grenoble Cedex* 9, *France. E-mail: thouve@obs.ujf-grenoble.fr*

[2]*Institut de Physique du Globe de Strasbourg (CNRS/ULP),* 5, *rue René-Descartes,* 67084 *Strasbourg, France*

Accepted 2003 May 5. Received 2003 April 23; in original form 2002 July 8

SUMMARY

In the French western Alps, east of Grenoble, we identify the Belledonne Border Fault as an active seismic fault. This identification is based on the seismic monitoring of the Grenoble area by the Sismalp seismic network over the past 12 yr (1989–2000). We located a set of earthquakes with magnitudes ranging from 0 to 3.5 along a ∼50 km long alignment which runs in a N30°E direction on the western flank of the Belledonne crystalline massif. Available focal solutions for these events are consistent with this direction (N36°E strike-slip fault with right-lateral displacement). These events along the Belledonne Border Fault have a mean focal depth of ∼7 km (in the crystalline basement), with a probably very low slip rate. The Belledonne Border Fault has never been mapped at the surface, where the otherwise heavily folded and faulted Mesozoic cover makes this identification difficult. Historical seismicity also shows that, over the past two and a half centuries, a few events located mainly along the southern part of the Belledonne Border Fault caused damage, with the magnitude 4.9 1963 Monteynard earthquake reaching intensity VII. The most recent damaging event in the study area is the magnitude 3.5 1999 Laffrey earthquake (intensity V–VI). Although its epicentre lies at the southern tip of the Belledonne Border Fault, there is clear evidence that aftershocks were activated by the left-lateral slip of a N122°E-striking fault. The length of the Belledonne Border Fault, which could easily accommodate a magnitude 6 event, as well as the proximity to the Isère valley with its unlithified Quaternary deposits up to 500 m thick known to generate marked site effects, make the identification of the Belledonne Border Fault an important step in the evaluation of seismic risk in the Grenoble area. Besides, the activity observed on the fault will now have to be taken into account in future geodynamic models of the western Alps.

Key words: aftershocks, Belledonne, fault, seismicity, seismotectonics, western Alps.

1 INTRODUCTION

The western Alps proceed from the Europe–Africa collision and from the indentation of the European margin by the Adriatic promontory (e.g. Tapponnier 1977; Lemoine *et al.* 2000). The resulting seismicity is usually moderate: each year, only one event has an M_L (Richter) local magnitude higher than 3.5, but slight to moderate damage to buildings can happen every 2–3 yr, due to the high population density in some parts of the region, and to site effects induced by loose sediments in glacial valleys. For these reasons, $M_L >$ 5 events—although they occur only a few times a century—can be quite destructive.

At the end of the 1980s, whereas seismic networks in Italy and Switzerland correctly monitored the regional seismicity, there were only a few isolated stations in the French western Alps. The 44-station Sismalp network was designed 15 yr ago to fill this gap (Thouvenot *et al.* 1990; Thouvenot 1996). Most instrumental seismicity concentrates along the French–Italian border where it forms the two Briançonnais and Piedmont seismic arcs as postulated by Rothé (1941) based on accounts of historical events. Sue (1998) achieved a detailed epicentre mapping of this region, while the corresponding stress field was thoroughly studied by stress inversion of the many focal mechanisms Sismalp made available (Sue *et al.* 1999). The inner part of the Alpine belt was clearly shown to be under radial extension.

Sismalp also aimed at discovering hitherto unknown active seismic zones, but the scarcity of earthquakes elsewhere in the Alpine foreland made such identifications difficult. Earthquakes seemed to happen there sparsely at random, without any clear interconnection. However, since 1992 when an $M_L = 2.3$ event occurred a few kilometres east of Grenoble, we have suspected the presence of an active fault in that place, on the northwestern flank of the Belledonne massif. Year after year, we gathered more and more evidence of its activity, also supported by historical records. With a few events of

magnitude between 0 and 2 per year, this activity was important enough to prompt us to install four temporary seismic stations in 1997 December, in addition to the permanent network. As no segment of the fault seemed more active than the others, these four stations were installed in line along the Belledonne massif. The seismic activity was weaker than usual in 1998, until 1999 January, when an $M_L = 3.5$ earthquake occurred at Laffrey at the southwestern tip of the fault, a few kilometres south of one of the temporary stations.

Because of its proximity to Grenoble and its 450 000-inhabitant conurbation, the Belledonne Border Fault (BBF) is of utmost importance in the evaluation of the seismic risk in the Grenoble basin. As such, it deserves a special review, which is the aim of this article. We will discuss the tectonic setting, the analysis of historical records and instrumental seismicity along the BBF, and conclude by addressing the Laffrey earthquake and its aftershock sequence which have unexpectedly lasted for several months.

2 TECTONIC SETTING

In the western Alps, NE of Grenoble, the Belledonne massif (Fig. 1) is the longest of the crystalline massifs that build up the L-shaped pattern of the External Crystalline Massifs: Aar, Gothard, Aiguilles Rouges, Mont Blanc and Belledonne (long leg), Pelvoux and Argentera (short leg). Extending over about 100 km in a straight NE–SW direction, the Belledonne massif was part of a Variscan orogen situated along a margin of the old European platform. During the Alpine orogenesis, crustal shortening commenced in the internal Alps 60 Ma and reached the external domain 20–30 Ma, uplifting parts of the Variscan basement and thus generating the

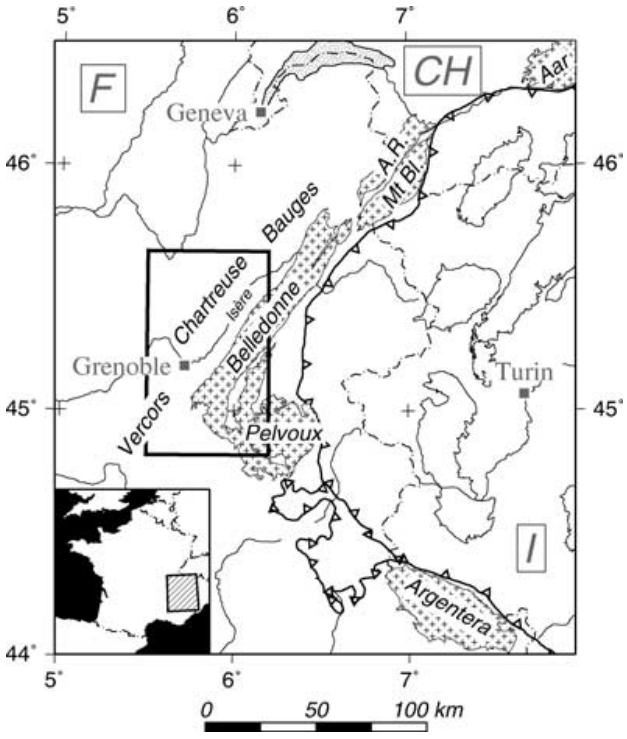

Figure 1. Schematic map of the western Alps, with the external crystalline massifs (cross pattern) and the Penninic Frontal Thrust (heavy line). CH = Switzerland; F = France; I = Italy; A. R. = Aiguilles Rouges; Mt Bl. = Mont Blanc. The box shows the study area.

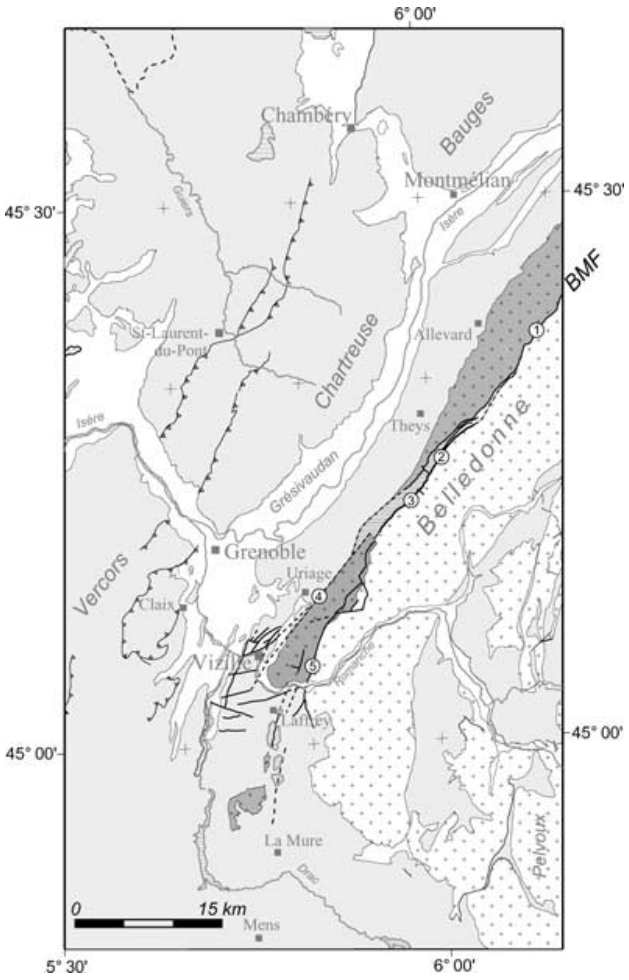

Figure 2. Simplified tectonic map of the study area. Blank = Quaternary deposits; shaded = Mesozoic and Cenozoic; cross pattern = Belledonne *Rameau interne*; dark cross pattern = Belledonne *Rameau externe*; horizontally hatched pattern = Belledonne Carboniferous Band. The Belledonne Middle Fault (BMF) is subdivided into five segments: 1 = Northern BMF; 2 = Eastern Merdaret Pass Fault; 3 = Pré de l'Arc Fault; 4 = Vizille Fault; 5 = Séchilienne Fault. Only faults related to the BMF are shown here; refer to Fig. 4 for a complete fault mapping.

Belledonne massif. This tectonic episode also deformed the Mesozoic cover, which was transported to the NW into a more external position where it now forms the Bauges, Chartreuse and Vercors Subalpine chains. The Chartreuse massif is separated from the Belledonne massif by the huge topographic depression of Grésivaudan (the Isère valley). The study area shown by Fig. 2 extends from 5°30′ to 6°12′E, and from 44°49′ to 45°39′N. It covers the southwestern part of Belledonne, the northwestern part of Pelvoux, the Grésivaudan, Chartreuse and parts of Vercors and Bauges. For this specific region, there is no tectonic synthesis available which the reader could be referred to. Since this article deals with a seismic alignment and discusses its relation to documented faults, the presentation of such a setting is necessary, even if connections between seismicity and tectonics will eventually prove very loose. Only the main features pertaining to the Belledonne massif, its sedimentary cover and the position of the pre-Triassic basement will be presented here.

The Belledonne massif is divided by the Belledonne Middle Fault (*Accident médian*), a presumably Variscan extension fault which

runs along its whole length (Fig. 2). The Belledonne Middle Fault (BMF) is, with the Nîmes Fault and the Cévennes Fault, one of the main N50°E–N60°E-trending Variscan fault zones that run through southeastern France. It has been suggested that the Nîmes Fault and the Cévennes Fault are presently active (Grellet *et al.* 1993; Lacassin *et al.* 1998). However, neither is supported by reliable instrumental-seismicity data. Further to the NE, the BMF probably merges into the Chamonix valley, which separates the twin massifs of Aiguilles Rouges and Mont Blanc.

The strike of the BMF is not exactly the same as the trend of the Belledonne massif, so that the fault is fairly close to the western border of the massif in the south, and more internal in the north (Fig. 2). The BMF separates the so-called *Rameau externe* (literally 'external branch'), made of micaschists, from the *Rameau interne* (gneiss, amphibolites and gabbros). From the north of the Belledonne massif down to 45°20′N latitude, the BMF corresponds to a single fault (labelled 1 in Fig. 2), which brings into contact the *Rameau externe* and the *Rameau interne*, with thin slices of Triassic 'cargneules' in places. Further south, down to the latitude of Grenoble (45°10′N), the BMF turns into a 15 km long, 2 km wide zone of large, mainly Carboniferous tectonic slices and therefore called the *Bande houillère* (Carboniferous Band) by Barféty *et al.* (2000). The eastern edge of this band is made of segments 2 and 3 of the BMF (Fig. 2), both steeply dipping to the east. The western edge is covered by a large area of thick glacial deposits, which makes its mapping uncertain; this complex fault zone is also suspected to dip steeply to the east.

South of the latitude of Grenoble, the Carboniferous Band disappears and the continuation of the BMF is unclear. It probably splits off into two branches. The N45°E-striking Vizille Fault (segment 4) stretches in a straight line to Vizille. It forms the contact between the *Rameau externe* and its Mesozoic cover, which distinguishes that fault from segments 1–3 described previously. Barféty & Gidon (1996) and Gidon (1998–2002) proposed that the Vizille Fault acted as a dextral strike-slip fault system which splits to the SW into a bunch of subfaults; however, this strike-slip movement remains hypothetical, since it is supported only by a few mapped outcrops. The Séchilienne Fault (segment 5) separates the *Rameau externe* from the *Rameau interne*, in a position similar to that of segment 1 further north. It crosscuts the Romanche valley and can be mapped up to the east of Laffrey. There are also hints that it continues further south (dashed line between Laffrey and La Mure in Fig. 2).

Overlooking the Grésivaudan, NW-facing Lower-Mesozoic border hills (*Collines bordières*) cover the lower slopes of the Belledonne massif (Uriage, Theys and Allevard localities in Fig. 2). This marly and calcareous Dogger series is separated from the Liassic and Triassic beds by an Aalenian soft argillite monocline forming a kind of bench along the massif (*Balcon de Belledonne*).

In the border hills, anticlines trend N15°E–N30°E, while a number of hypothetical, mainly dextral, strike-slip faults striking N50°E–N65°E have been proposed by Barféty & Gidon (1996). It is difficult to rely on the existence of these faults in most of the study area. The tectonics of the border hills remain complex to decipher, mainly because the Bajocian and Aalenian series do not allow faults to leave clear imprints. What can be retained is: (1) there is no evidence that folds and faults in the border hills are related to deep crustal faults; (2) field observations document dextral strike-slip in several places, even if the identification of continuous N50°E–N65°E faults is controversial; and (3) these faults, where recognized, formed later than the folding of the border hills.

The basement position beneath the Subalpine chains and the border hills is poorly documented. The ECORS-CROP seismic reflection profile, much further north, yielded a maximal value of 4 km beneath the Bornes massif (Guellec *et al.* 1990), with a rather smooth rise of the basement towards the Belledonne massif. In contrast, Thouvenot & Ménard (1990) interpreted explosion-seismology data in the Chartreuse massif and proposed a model with a 9 km deep basement panel overlaid by a 3 km deep flake, with the overthrust of the Belledonne massif on top of that. Recently, Deville & Chauvière (2000) reprocessed seismic reflection data in approximately the same area to compute a 6 km deep autochthonous basement and a Belledonne massif made of two superposed frontal wedges.

3 INSTRUMENTAL SEISMICITY

The first stations of the Sismalp seismic network were installed in 1987–1988. Our instrumental-seismicity database begins in 1989 and ends on 2000 December 31. The 44-station Sismalp network was completed in 1994 only, so that there are few events located in the study area at the beginning of the database. We have not included instrumental data prior to 1989 in our catalogue, because at that time there were only at most two permanent seismic stations operating in the study area itself, in comparison with seven stations operating now (Fig. 3a): six Sismalp stations and one LDG station (Laboratoire de Détection et de Géophysique, CEA, Bruyères-le-Châtel). In 1997 December, we installed four additional stations along the northwestern flank of the Belledonne massif, and, in late 1999 January, four more stations in the $M_L = 3.5$ 1999 Laffrey earthquake epicentral zone. These eight temporary stations were kept operating until 1999 May. All permanent and temporary stations are equipped with digital recorders. The Sismalp permanent stations were fitted with one-component 1 Hz seismometers, while the LDG station and the temporary stations were fitted with three-component seismometers.

When available, we merged arrival times from other seismic networks: LDG, RéNaSS (Réseau National de Surveillance Sismique, Strasbourg), SED (Schweizerischer Erdbebendienst, Zurich) and IGG (Istituto Geofisico e Geodetico, Genoa). The whole database was reprocessed to control picked arrival times using the Pickev 2000 software developed at the Observatoire de Grenoble (Fréchet & Thouvenot 2000), which allows interactive picking and preliminary locations.

Earthquakes were thereafter located with a modified version of the Hypo71 program (Lee & Lahr 1975) that includes elevation corrections and takes into account secondary arrivals (Fréchet & Glot, private communication, 1984). At that stage, we used a four-layer 1-D velocity model (Table 1) derived from Fréchet (1978). Such a crude model might seem inadequate for the western Alps, but a more sophisticated model is not presently available: the 12-layer 1-D velocity model computed by Sellami *et al.* (1995) is valid for the internal zones of the chain, whereas local-earthquake tomographic images by Solarino *et al.* (1997) or by Paul *et al.* (2001) are centred on those internal zones where most seismic activity concentrates, which excludes the Grenoble area. In the model of Table 1, based on rare deep-seismic-sounding data, the 3 km thick top layer with a velocity of 5.3 km s^{-1} can represent both the weathered micaschist

Table 1. 1-D velocity model used for locating earthquakes.

Velocity (km s^{-1})	Depth to the top of the layer (km)
5.30	0
5.92	3
6.60	27
8.00	35

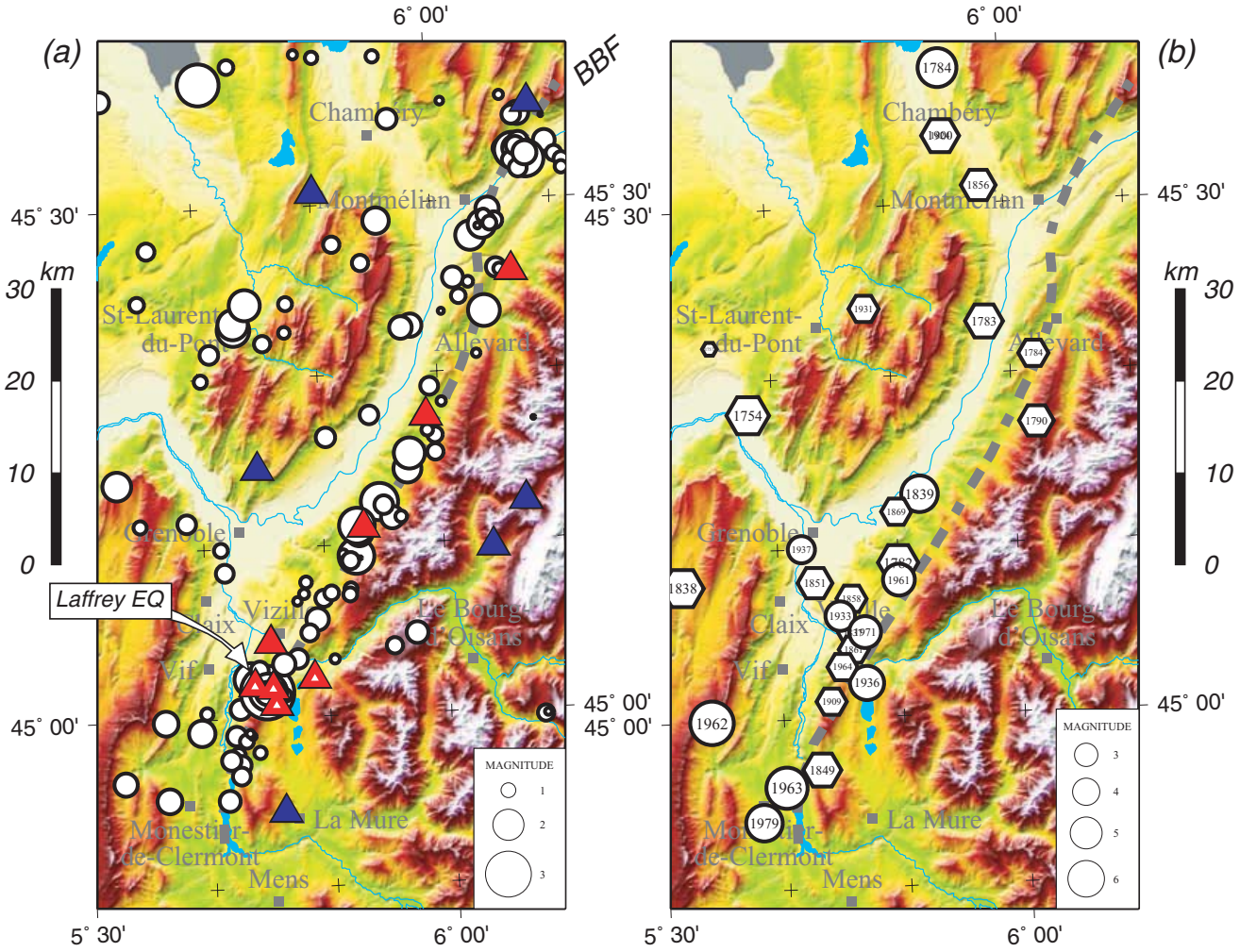

Figure 3. Seismicity maps of the study area. (a) Instrumental seismicity for the 1989–2000 period, with seismic stations shown by triangles (blue, permanent; red, BBF experiment (December 1997–May 1999); red and white, Laffrey aftershock monitoring (January–May 1999)); (b) revised historical seismicity for the 1356–1988 period (circles = quality A–C; hexagons = quality D); magnitude scale approximate: maximum intensities converted to magnitude using the relation $M = 0.44\ I_m + 1.96$ derived from Levret *et al.* (1996). BBF = Belledonne Border Fault.

or gneissic basement and the massive coral-reef limestone series of the Subalpine chains (Thouvenot 1981). However, it is clear that we are presently lacking a 3-D model or at least a finer 1-D model, which would improve location accuracy.

M_L magnitudes were computed for each event by measuring the ground peak displacement for all available digital signals and by averaging the individual values. Finally, we checked each event against a database containing typical records of known quarry shots in the study area, in order to clear man-made events. This selection is crucial because there are many quarries in the Grenoble area. One event out of two in our initial catalogue proved to be of artificial origin. The raw catalogue (439 events) shows an unquestionable increase for weekdays and for the 09:00–17:00 local time period. Most events occur between 10:00 and 12:00 local time, known to be a favourite shooting window for local quarriers. In contrast, the cleared catalogue (181 earthquakes) yields quasi-random distributions with regard to weekdays and local time. We also excluded from the catalogue several events corresponding to landslides or rock avalanches.

Of the 181 earthquakes, we kept only events for which at least six arrival times had been read and for which a horizontal epicentral uncertainty smaller than 10 km had been estimated. For these 163 earthquakes, we compute a 5 ± 3.5 km mean focal depth, in accordance with what Deichmann (1992) found for the seismicity of the Helvetic nappes and the Aar-Gothard massifs in Switzerland. However, in contrast with Deichmann's results for the Molasse basin, deep events are rare. The deepest one (20 ± 2 km) is an $M_L = 0.9$ earthquake which occurred in 1997 in the Vercors massif, due west of Grenoble. In our catalogue, although the mean number of arrival times available for a given event is high (23), the mean azimuthal gap and the mean minimum epicentral distance are still large (130° and 13 km); however, the low mean rms residual (0.25 s) ensures mean horizontal and vertical uncertainties of 1.1 and 2 km, respectively. Although we noted the large proportion of quarry shots in the initial catalogue, we could not use them to check the location uncertainties because: (1) those quarry shots are exclusively located to the NW of Grenoble, a zone on the fringe of the study area; (2) those events have low magnitudes (around 1) and do not provide signals usable for that kind of investigation.

Instrumental seismicity as plotted in Fig. 3(a) demonstrates a SSW–NNE-trending alignment, which moulds to the western flank of the Belledonne massif from the south of Vizille to Allevard.

Strictly speaking, we should use the 'alignment' terminology, and name it the 'Belledonne Border Seismic Alignment'. However, this seismic lineation cannot be explained without postulating a fault zone at depth, even if the 'fault' terminology is usually reserved for a tectonic feature duly identified at the surface. To be more succinct, the seismic alignment will be henceforth named the 'Belledonne Border Fault', although 'Belledonne Border Fault Zone' would have been more correct, as available data do not allow us to distinguish a single fault from a fault zone.

From Fig. 4, where instrumental seismicity is plotted on to the tectonic map of the study area, we observe that the BBF might correspond to the contact between the *Rameau externe* and its Mesozoic cover for a mere 7.5 km NE of Vizille. From Uriage to Theys, where the BBF is best defined by several events with magnitudes between 2 and 3, the seismic alignment becomes more external, with foci beneath the Mesozoic cover of the *Rameau externe*, with no corresponding fault at the surface. The BBF is therefore not to be mistaken for the BMF, except for the 7.5 km section mentioned above (part of segment 4 in Fig. 4).

Between the south of Vizille and Theys, where the most active section of the fault trends N30°E, the narrowness of the seismic alignment suggests that the BBF is vertical. When selecting best-located events, we find a mean focal depth of 7 ± 3 km. We also note that the N30°E strike of the BBF along the Belledonne massif is different from the N50°E–N65°E strike found by Barféty & Gidon (1996) for the dextral strike-slip faults they claim to have observed in the border hills.

The continuation of the BBF to the NE is unclear: the seismicity is located away from the border hills and clusters in the Isère valley south and NE of Montmélian, with no known faults reported (Fig. 4). Another cluster of three events located along the northwestern border of the Chartreuse massif close to St-Laurent-du-Pont and an isolated $M_L = 2.8$ earthquake further north show that the Alpine seismicity extends to the NW much further than the Subalpine chains themselves.

South of Vizille, in the Laffrey area, the seismic alignment of the BBF abuts on a small transverse fault (Brion Fault), precisely in a place where the Belledonne massif veers to the SE to join the Pelvoux massif. In that place, the seismicity seems to shift to the west, and follows a more N–S direction, along the Drac valley and the western flank of the La Mure crystalline dome, a southern extension of the *Rameau externe*. A few events located further west in the Vercors massif make such a southward continuation of the BBF debatable. The BBF might actually splay out into two branches: a N–S branch along the Drac valley and a still speculative NNE–SSW branch across the Vercors massif. It might be significant—as will be seen in Section 5—that the Laffrey area, where we noted a complication in the BBF geometry brought about by the presence of the Brion Fault, corresponds to the epicentral zone of the largest earthquake we ever located in the study area over the last 12 yr.

4 HISTORICAL SEISMICITY

The earliest seismic events possibly having their epicentres in the study area date back to the second half of the 14th century (Table 2). Nevertheless, the evidence for these earthquakes is very slight, because it does not rely on a direct account, but rather on brief mentions in two books published more than 300 yr later (Chorier 1672; Allard *ca.* 1710). The next events occurred much later, at the turn of the 17th century; they rely on contemporaneous sources, but are not much better known. The period for which epicentres can be estimated with some confidence begins in the mid 18th century with the 1754 Voreppe earthquake.

Rothé (1941) compiled the first catalogue of western Alps seismicity that included epicentral estimates. It was mainly based on Alexis Perrey's work for events prior to 1872, and on research performed by Rothé and others at the Institut de Physique du Globe in Strasbourg (IPGS) for subsequent years. It is not known whether they used the unpublished catalogue of Montessus de Ballore (1905) for the 1872–1905 period. More recently the French seismotectonic mapping project (Vogt 1979; Lambert 1997) completely revisited the historical seismicity of France. The associated database (Sirene) is not public, but a partial catalogue was published (Lambert & Levret-Albaret 1996), which lists all events with intensity larger than or equal to MSK V–VI.

Our own research showed that many smaller events were not thoroughly investigated in these catalogues and that new data could be gathered, especially from local newspapers in the 1774–1919 period. The first local newspaper in Grenoble (*Affiches de Dauphiné*) was launched in 1774, while the IPGS was founded in 1919 and the BCSF (Bureau Central Sismologique Français) in 1921. This prompted us to revise the historical seismicity thoroughly. Previous compilations and catalogues were gathered (Billiet, Cotte, Gueneau de Montbeillard, Montessus de Ballore, Perrey, Rothé, Sirene, Villard, Von Hoff, etc.), which allowed us to produce a complete list of dates and places. Original sources were then systematically searched for all events before 1919 with intensity smaller than MSK VI and for some larger events. Many new sources were found during that stage. For larger events or events after 1918, we mainly relied on results published by IPGS/BCSF or Sirene investigations. Recently, as this work came close to its end, the Sirene group provided a more extensive version of their database on the so-called 'SisFrance' World Wide Web site (SisFrance 2002). A comparison with the SisFrance database demonstrated the completeness and accuracy of our catalogue.

Table 2 presents the revised historical catalogue of epicentres located in the study area. It also includes a few very poorly constrained earthquakes when we suspected them to have their epicentres in the study area. The catalogue brings out several new epicentres and also corrects errors found in previous works. It contains 92 events: 54 mainshocks, six foreshocks, 27 aftershocks and five swarms. Events since 1989 are not included because they have been considered in the instrumental seismicity study (Section 3). More than 25 erroneous earthquakes were identified (wrong dates, wrong locations or non-seismic events) and removed from or corrected in the database. The maximum intensity, when available, is estimated using the MSK scale. The quality of the epicentre location is rated with a code ranging from A (a few kilometres) to D (up to 50 km of uncertainty). Some events have a highly hypothetical location; when given, their coordinates are only for documentation, and their location quality is rated E. Epicentres of large earthquakes are not necessarily more reliable because small earthquakes are felt in a very small radius, and their epicentres can often be pinpointed with good accuracy. Nevertheless, we generally assigned quality D to these small earthquakes because historical sources available to us are usually too limited to prove that the earthquake was not felt elsewhere.

Fig. 3(b) shows all epicentres of Table 2, excluding foreshocks, aftershocks and quality-E events. The striking feature on this map is the alignment of foci along the western border of the Belledonne massif, in a position very close to that of the BBF (compare with Fig. 3a). The alignment is very clear between Monestier-de-Clermont to the SW and Allevard to the NE. The rest of the historical seismicity is scattered in the Subalpine massifs (Vercors and

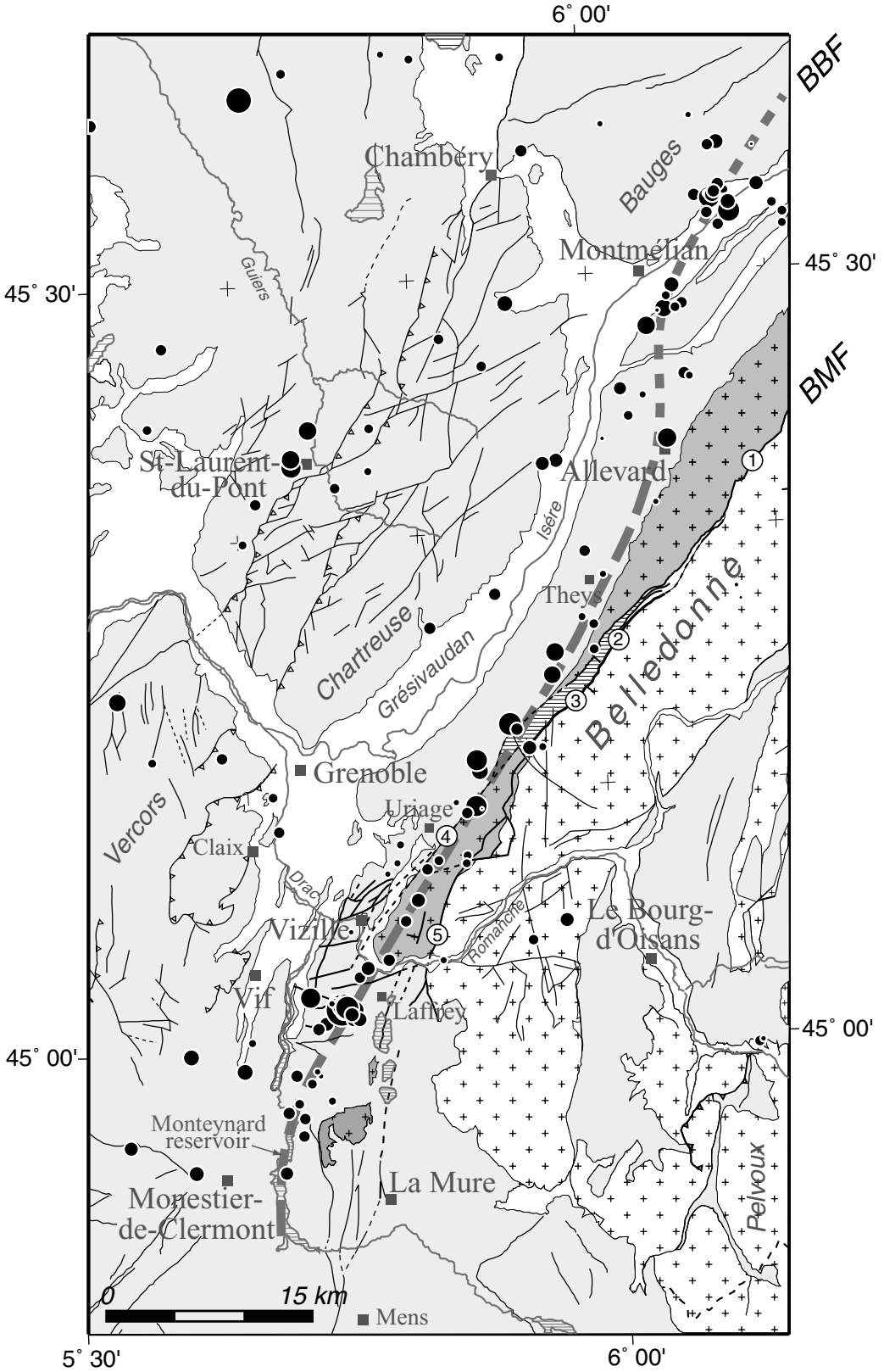

Figure 4. Tectonic map of the study area with instrumental seismicity for the 1989–2000 period. Blank = Quaternary deposits; shaded = Mesozoic and Cenozoic; cross pattern = Belledonne *Rameau interne*; dark cross pattern = Belledonne *Rameau externe*; horizontally hatched pattern = Belledonne Carboniferous Band. BBF = Belledonne Border Fault. The Belledonne Middle Fault (BMF) is subdivided into five segments: 1 = Northern BMF; 2 = Eastern Merdaret Pass Fault; 3 = Pré de l'Arc Fault; 4 = Vizille Fault; 5 = Séchilienne Fault.

Table 2. Revised historical catalogue for the study area. Q = epicentre quality (Sirene classification): uncertainty A = less than a few kilometres, B = about 10 km, C = between 10 and 20 km, D = between a few kilometres and 50 km, E = epicentral coordinates given for information only; Im = maximum MSK intensity; N = number of localities where the earthquake was reported felt; + means that the earthquake was also reported felt in other unidentified neighbouring localities; T = earthquake type (Sirene classification): P = foreshock; R = aftershock; Z = swarm.

Date	Time	Lat. N	Lon. E	Q	Im	N	T	Location
. .1356				E		1+		Grésivaudan ?
. .1377				E		1+		Grenoble ? Mens ?
. .1379		45°11′	5°43′	E		1		Grenoble
. .1691		45°11′	5°43′	E		1		Grenoble
.12.1721		45°11′	5°43′	E		1		Grenoble
13.08.1733	06:	45°37′	6°08′	E		1		St-Pierre-d'Albigny
	16:	45°37′	6°08′	E		1		St-Pierre-d'Albigny
12.01.1754	23:30:	45°18′	5°38′	D	6.5	3		Voreppe
15.09.1757	23:30:	45°22′	5°35′	D		4		Voiron
15.08.1782	16:	45°09′	5°50′	D	6.0	2		Uriage
05.05.1783		45°11′	5°43′	E		1	Z	Grenoble
21.06.1783	18:	45°23′	5°58′	D	5.5	1+		Montalieu
	21:	45°23′	5°58′	D		1+	R	Montalieu
15.10.1784	12:03:	45°38′	5°55′	C	6.5	25		Aix-les-Bains
03.12.1784	16:	45°21′	6°02′	D	4.0	3	Z	Theys
. .1788		44°58′	5°42′	E		1		Monteynard
02.11.1789	11:55:	45°22′	5°47′	E		1		Chartreuse
. .1790				E				Maurienne
02.01.1790	12:	45°17′	6°02′	D	5.0	3		Theys
07.07.1791	06:	44°58′	5°42′	E	4.0	1		Monteynard
13.02.1809	21:30:	45°11′	5°43′	E		1		Grenoble
29.10.1824	20:	45°34′	5°55′	D	4.0	1+		Chambéry
29.01.1837	13:50:	45°05′	5°46′	D	4.0	1		Vizille
22.05.1838	07:	45°08′	5°32′	D	6.5	1		Méaudre
03.04.1839	18:37:	45°13′	5°52′	C	6.0	10		Le Versoud
27.04.1842	13:	45°11′	5°43′	E	3.5	1		Grenoble
07.01.1844	09:22:	45°34′	5°55′	E	4.0	1		Chambéry
03.08.1849	22:25:	44°57′	5°43′	D	5.5	7		La Motte-d'Aveillans
07.01.1851	23:22:	45°08′	5°43′	D	5.0	3		Echirolles
17.05.1856	16:25:	45°31′	5°58′	D	5.0	6		Myans
12.04.1858	04:	45°11′	5°43′	E	4.0	1		Grenoble
08.07.1858	15:	45°07′	5°46′	D	4.0	3		Uriage
28.12.1858	06:30:	45°34′	5°55′	E		1		Chambéry
28.07.1861	23:	45°04′	5°46′	D	4.0	3		Vizille
12.11.1869	00:02:	45°12′	5°50′	D	4.0	3		Domène
13.11.1869	00:31:	45°12′	5°50′	E		2	R	Domène
14.11.1869	21:05:	45°12′	5°50′	E		1	R	Domène
09.02.1876	02:50:	45°34′	5°55′	E	4.5	1	Z	Chambéry
08.11.1882	23:30:	45°19′	5°58′	E		1		Tencin
06.01.1885	03:30:	45°34′	5°55′	E		1		Chambéry
15.02.1885	22:	45°34′	5°55′	E		1		Chambéry
25.12.1900	23:20:	45°34′	5°55′	D	5.5	1+		Chambéry
08.12.1905	09:43:10	45°11′	5°43′	E		1		Grenoble
18.02.1909	10:13:	45°01′	5°44′	D	4.0	3+		Notre-Dame-de-Commiers
06.01.1911	03:	45°11′	5°43′	E	3.0	1+	Z	Grenoble
11.09.1931	22:30:	45°24′	5°48′	D	4.0	4		E. St-Laurent-du-Pont
07.11.1933	09:48:40	45°06′	5°45′	B	4.5	10		Champagnier
30.01.1936	18:45:	45°02′	5°47′	B	5.5	22		Uriage
17.01.1937	01:	45°10′	5°42′	B	4.0	14		Grenoble
25.03.1953	03:29:	45°22′	5°47′	E	3.0	2		St-Pierre-de-Chartreuse
22.07.1954		45°04′	4°50′	E		1		Tournon
02.12.1955	19:55:	45°19′	6°05′	E		1		La Ferrière
	23:	45°19′	6°05′	E		1		La Ferrière
03.03.1961	00:52:27	45°08′	5°50′	A	5.0	63		Uriage
12.04.1962	13:38:05	45°02′	5°34′	B	5.0	32	P	Corrençon-en-Vercors
	20:12:00	45°02′	5°34′	D	4.5	7	P	Corrençon-en-Vercors
	20:18:26	45°02′	5°32′	E		4	P	Corrençon-en-Vercors
23.04.1962	00:33:25	45°02′	5°34′	E		3	P	Corrençon-en-Vercors
25.04.1962	04:44:48	45°00′	5°34′	A	7.5	471		Corrençon-en-Vercors
27.04.1962	04:17:43	45°00′	5°34′	D	5.0	23	R	Corrençon-en-Vercors

Table 2. (*Continued.*)

Date	Time	Lat. N	Lon. E	Q	Im	*N*	T	Location
24.05.1962	02:40:	45°00′	5°33′	E			R	Corrençon-en-Vercors
28.05.1962	16:21:27	45°00′	5°33′	B	5.0	14	R	Corrençon-en-Vercors
07.06.1962	19:55:15	45°01′	5°34′	C	5.0	14	R	Corrençon-en-Vercors
15.07.1962	04:36:11	44°57′	5°36′	C	5.0	8	R	Corrençon-en-Vercors
21.04.1963	21:30:	45°02′	5°32′	E		1	P	Monteynard
	01:35:	44°55′	5°38′	E		1	Z	Monteynard
25.04.1963	13:36:11	44°56′	5°40′	A	7.0	151		Monteynard
	20:24:19	44°58′	5°42′	E	3.0	31	R	Monteynard
	23:	44°58′	5°42′	E	2.0	5	R	Monteynard
	23:58:	44°58′	5°42′	E		3	R	Monteynard
27.04.1963	05:28:20	44°56′	5°39′	B	7.0	57	R	Monteynard
30.04.1963	05:20:	44°57′	5°41′	E		1	R	Monteynard
01.05.1963	02:56:40	44°57′	5°41′	E		1	R	Monteynard
23.10.1963	06:09:22	44°58′	5°40′	E	2.5	4	R	Monteynard
02.12.1963	06:03:	44°56′	5°40′	D	4.0	7	R	Monteynard
04.12.1963	11:26:42	45°02′	5°35′	B	6.0	33	R	Corrençon-en-Vercors
07.12.1963	10:39:	45°00′	5°33′	C	6.0	14	R	Corrençon-en-Vercors
12.12.1963	13:24:57	45°03′	5°31′	C	6.0	12	R	Corrençon-en-Vercors
	17:23:55	45°00′	5°34′	E		5	R	Corrençon-en-Vercors
17.12.1963	17:31:44	45°00′	5°34′	E		2	R	Corrençon-en-Vercors
20.12.1963	07:09:	44°58′	5°41′	E		1	R	Monteynard
26.12.1963	06:13:	44°58′	5°41′	E		2	R	Monteynard
21.07.1964	02:41:25	45°39′	5°54′	E	3.5	8		Viviers-du-Lac
13.08.1964	05:18:41	45°03′	5°45′	D	4.0	16		Vizille
05.10.1964	15:15:51	45°08′	5°35′	E	3.5	9		Lans-en-Vercors
01.11.1964	04:57:	44°58′	5°42′	E		2	R	Monteynard
02.05.1965	12:25:43	44°58′	5°42′	E		1	R	Monteynard
24.08.1966	20:47:04	44°59′	5°42′	C	5.0	11	R	Monteynard
14.01.1971	03:05:44	45°05′	5°47′	B	5.0	60		Vizille
22.11.1979	06:26:49	44°54′	5°38′	D	4.0	19	P	Monteynard
	07:24:07	44°54′	5°38′	A	6.0	65		Monteynard
21.12.1979	13:52:	44°58′	5°41′	E		2	R	Monteynard

Chartreuse). To the SE, the external crystalline massifs of Belledonne and Pelvoux appear completely aseismic.

The two largest damaging earthquakes struck in 1962 and 1963. The $M_L = 5.3$ Corrençon earthquake of 1962 April 25 occurred in the northeastern part of the Vercors massif, definitely not on the BBF alignment. It reached a maximum MSK intensity of VII–VIII, with severe damage to several villages but fortunately without death toll. Exactly 1 year later, on 1963 April 25, a few kilometres to the SE, the $M_L = 4.9$ Monteynard earthquake struck at the southwestern end of the BBF alignment, with a maximum intensity of VII. The alignment comprises about 18 epicentres, spanning from 1782 to 1979. The most active part of the alignment is its southwestern half, between Monestier-de-Clermont and Uriage: intensity VII occurred during the aforementioned 1963 April 25 earthquake in 13 villages around the Monteynard reservoir; intensity VI was reached on 1782 August 15 at Uriage, on 1839 April 3 in seven villages around Le Versoud, and on 1979 November 22 at Marcieu and Treffort; intensity V–VI was reached on 1849 August 3 at La Motte-Saint-Martin, and on 1936 January 30 at Laffrey. The northeastern part of the BBF alignment, between Uriage and Allevard is less active; the highest intensity did not exceed V, e.g. on 1784 December 3 and on 1790 January 2 at Theys.

Some earlier, possibly large, events are not plotted on this map because their macroseismic epicentres are debatable. During the 14th century, three or four damaging earthquakes are mentioned by later works (Chorier 1672; Allard *ca.* 1710; Villard 1887). They caused damage in Grésivaudan and Trièves (the region south of La Mure), with the cities of Grenoble and Mens supposedly suffering strong damage. Although the 1356 event—the earliest event in the catalogue—could be the famous Basle earthquake, it could also be a strong local earthquake, since the Basle earthquake most probably did not exceed intensity III in Grésivaudan (see, e.g., Lambert 1997). Because we do not know yet of any contemporaneous report for these 14th-century events, and because the sources cited above are rather vague, these earthquakes could also have taken place on the BBF or along an unknown active fault more to the south. They deserve special historical investigations which remain to be carried out.

5 THE $M_L = 3.5$ 1999 LAFFREY EARTHQUAKE

5.1 Mainshock

The strongest event on the BBF recorded in the last 12 yr ($M_L = 3.5$, Sismalp; $M_b = 3.4$, International Seismological Centre) struck at 03:36 UTC on 1999 January 11 (Bureau Central Sismologique Français 2002). It occurred 13 months after four temporary stations had been installed along the fault to monitor its activity, and 5 km south of the southernmost station (Fig. 3a). This could be considered a mere coincidence if these four stations had been installed there just to reduce the spacing between stations of the permanent network.

Table 3. Focal parameters of the Laffrey earthquake, using a routine location and a double-difference relocation. H_0 = date and origin time (UTC); Z = focal depth (km) relative to sea level; M_L = local magnitude; N = number of available P- or S-wave arrival times; G = azimuthal gap (deg); D = minimum epicentral distance (km); rms = rms residual (s); ERH = horizontal uncertainty (km); ERZ = vertical uncertainty (km).

	H_0	Lat. N	Long. E	Z	M_L	N	G	D	rms	ERH	ERZ
Preliminary routine location	990111 03:36:36.5	45°01.9′	5°46.3′	−0.8	3.5	38	102	13.1	0.2	0.6	0.8
Final double-difference relocation	**990111 03:36:36.4**	**45°01.5′**	**5°44.8′**	**2.9**	**3.5**	**129**	–	–	**0.3**	**0.3**	**0.4**

However, one should bear in mind that the 44-station Sismalp network, in allowing us to observe and locate low-magnitude events (typically any event of magnitude larger than 1.3), has focused our interest on this part of the Belledonne massif over a whole decade. Though the earthquake was in no way predicted, its occurrence was no surprise.

The earthquake was felt with a maximum MSK intensity of V–VI at three localities (SisFrance 2002): St-Georges-de-Commiers, Champ-sur-Drac and Claix (see Fig. 12 below), where characteristic damage was observed in wall masonry, cladding and covering. (Damage at Claix was rated VI by the Bureau Central Sismologique Français (2002).) These three localities are situated in the Drac valley, respectively, 4, 5 and 11 km to the W–NW of the epicentre, in a zone of Wurmian glacial deposits covered by post-Wurmian river deposits which obviously produced site effects. Nevertheless, the shock was felt as far as the Chartreuse massif, 30 km to the north (I = IV), or the Pelvoux massif, 30 km to the east (I = III). A macroseismic map was published by the Bureau Central Sismologique Français (2002).

24 stations with epicentral distances shorter than 75 km were selected for locating the earthquake. In this way, residuals are neither biased by a poorly known lower crustal structure nor by strong Moho depth variations affecting mantle phases. In a second stage, we used Waldhauser's (2001) technique to relocate the mainshock and the aftershocks recorded by both the permanent network and the temporary network (see details in Section 5.2). The relocation falls 2.1 km W–SW of the first estimate (Table 3). This difference in horizontal distance is much larger than the 600 m horizontal uncertainty initially computed, and this value is probably underestimated. We investigated this point using the master-event technique. We performed four different relative locations, successively using one of the four best-recorded aftershocks as the master event. When averaging these locations, the mainshock is found to have exactly the same epicentral coordinates as those obtained previously using the Waldhauser's (2001) technique; the focal depth is slightly shallower (2.5 versus 2.9 km). This strengthens the reliability of the second line of Table 3, which we consider as our final solution for the mainshock.

The hypocentre is located 3 km W–SW of Laffrey, beneath the Conest mountain, which corresponds to the Mesozoic parautochthonous cover of the *Rameau Externe*, east of the Drac valley (Figs 4 and 12). Liassic nodulous bluish limestones (*Calcaires de Laffrey*) outcrop there in a compact 200–300 m thick formation, while the underlying Triassic series is reported to be 50 m thick at most. Cross-sections of the La Mure coal basin by Gignoux & Moret (1952) show that the basement–cover interface is steeply dipping west from the Laffrey plateau towards the Drac valley. However, given the focal depth of 2.9 km (as referred to sea level, i.e. 4.3 km beneath the surface), we can safely conclude that the hypocentre was located in the upper part of the pre-Triassic *Rameau Externe* micaschist basement.

The focal mechanism was derived from the first-motion data recorded at 45 stations with good azimuthal coverage. The solution

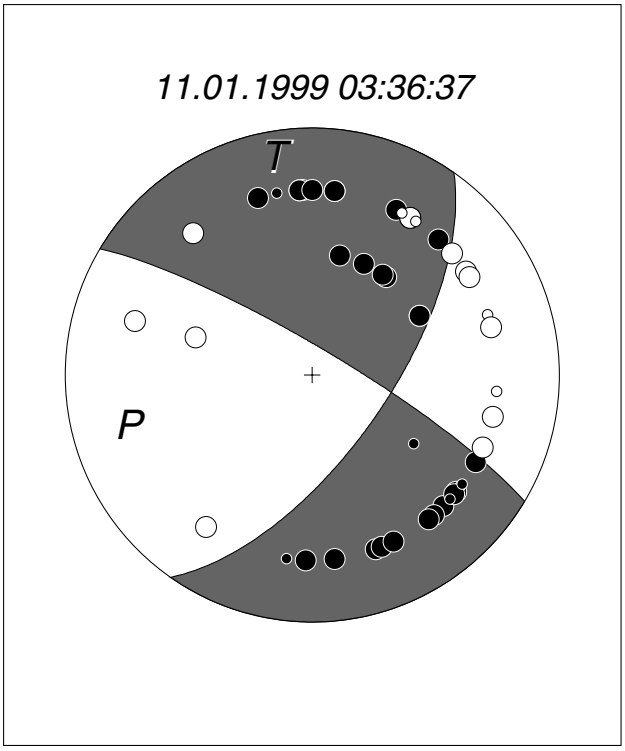

Figure 5. Focal mechanism of the Laffrey earthquake (lower hemisphere, Schmidt projection). Full symbols, compression; open symbols, dilatation; symbol size is smaller when first motion is emergent. Preferred fault plane strikes N120°E, with a 80°N dip.

is well constrained: it is a clear strike-slip mechanism (Fig. 5). The N35°E-striking nodal plane dips 65° to the SE, while the N120°E-striking plane dips 80° to the NE. This mechanism and those of other events along the BBF are discussed more thoroughly in Section 6. The strike of the first plane is close to that of the BBF from the south of Vizille to Allevard (N30°E). If that were the fault plane, this would mean a right-lateral strike-slip motion. However, the aftershock analysis below will demonstrate that rupture probably occurred within the other nodal plane, with a left-lateral strike-slip motion.

5.2 Aftershocks

Aftershock activity is difficult to predict after moderate-magnitude earthquakes, and we had not anticipated that such a low-magnitude shock would generate tens of aftershocks in the following months. The four temporary stations installed along the BBF in 1997 December, even with one station only 5 km from the epicentre, proved insufficient to monitor the early aftershocks correctly. Four more stations were installed in late January. During the 4 months

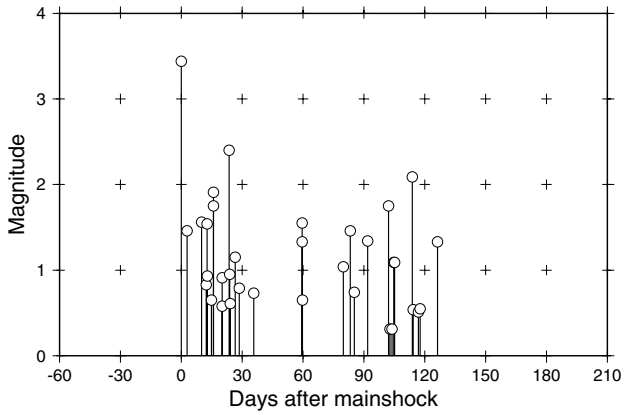

Figure 6. Time distribution of the Laffrey aftershocks. Each bar represents an earthquake; zero time corresponds to 1999 January 11.

after the mainshock, we located 33 aftershocks with magnitude ranging from 0.3 to 2.4. The strongest ($M_L = 2.4$) occurred on February 3, more than 3 weeks after the mainshock. The time distribution of aftershocks (Fig. 6) shows periods of activity followed by quiescence. The same phenomenon was observed following the 1996 $M_L = 5.3$ Annecy earthquake, which also generated a profusion of aftershocks over several years (Thouvenot *et al.* 1998). For both Laffrey and Annecy events, the focus was very shallow (2.9 and 2 km, respectively), and both had strike-slip mechanisms. Scholz (1990) already noted that aftershocks for strike-slip earthquakes commonly seem to be restricted to the rupture plane, which they define quite well. In addition, strike-slip mechanisms with shallow rupture planes may produce a lavish aftershock activity.

This section is dedicated to the relative position of the mainshock compared with the aftershocks. In the 42-event data set we used, we included three 'foreshocks' (in 1989, 1997 and 1998), the mainshock, 33 aftershocks (in 1999), and five late 'aftershocks' (in 2000). These terms need to be discussed. In the Laffrey aftershock zone, Sismalp has monitored only three events over the previous 8 yr. The largest magnitude is an $M_L = 2.2$ earthquake, which occurred on 1997 September 23 and is reported to have been felt at Vizille and Vif. Whether it is a foreshock is a moot point, because it preceded the mainshock by a large time span of 16 months. On the map of Fig. 4, this 'foreshock' is located a few kilometres to the NW of the Laffrey mainshock. After the aftershock sequence shown in Fig. 6, no seismic activity was recorded in the aftershock zone between 1999 May and 2000 March. From 2000 March to September, five events occurred, the strongest reaching an $M_L = 2.4$ magnitude on 2000 August 17, 19 months after the mainshock. During the 2000 March–September period, the seismic activity was much higher than before the mainshock, and one can wonder whether those five events were late aftershocks. This section will also try to answer this question.

Most aftershocks used in the data set were felt, with frequent reports from Saint-Georges-de-Commiers where some of them reached MSK intensity IV, and surprisingly almost none from Laffrey, a phenomenon probably due to the same site effects as those already noted for the main shock (Section 5.1). The lowest magnitude value (0.6) was reached for the January 31 08:03 event, which was felt again at Saint-Georges (MSK II), 5 km west of the computed epicentre.

To refine locations, we first selected stations with epicentral distances shorter than 75 km. The aftershock zone is E–W elongated (Fig. 7a), but its 5 km horizontal dimension is inconsistent with an $M_L = 3.5$ shock. We thereafter used Waldhauser's (2001) double-difference technique to relocate hypocentres: the 42-event set was considered a single cluster and we selected pairs of earthquakes that were linked by at least eight phase pairs (see Waldhauser & Ellsworth 2000, for details of the technique). The singular-value decomposition normally suitable for small data sets proved unstable, perhaps because events were too weakly linked. We used the conjugate-gradients method instead, which converged efficiently and allowed us to relocate 80 per cent of the earthquakes. Most relocated events (Fig. 7b) collapse into a ∼1.2 km long segment (Fig. 7e), which trends N122°E (±2°). This prompted us to choose the N120°E-striking plane of the focal mechanism as the fault plane (Fig. 5), with a left-lateral strike-slip motion. In the geological fault pattern of Figs 7(b) and (e), the Brion Fault is almost coincident with the N122°E-trending seismic alignment. Its strike (N112°E) is very close to the N122°E and N120°E values ascertained above. The 10° strike discrepancy and the ∼500 m horizontal offset between the Brion Fault and the N122°E alignment can be ascribed to the difficulty of mapping the fault in the field, to its dip which is unconstrained, and to the uncertainty on the position of the cluster centroid.

A cross-section along the N122°E direction (Fig. 7c) shows a 55° NW-dipping seismic zone, between 1.6 and 3 km below sea level. Such a feature *cannot* be ascribed to the effect of a decollement of the Mesozoic cover on its pre-Triassic basement, a phenomenon frequently encountered in the western Alps where the Triassic series is rich in evaporites: the basement is expected above sea level in this zone (*cf.* the above discussion on the focal depth of the mainshock), not at a 2 km depth. Across the fault plane (Fig. 7d), the aftershock zone is imaged as a near-vertical band, in agreement with the 80° dip given by the focal mechanism. The rupture surface mapped by the aftershock zone is a narrow, 0.3 km wide, 2 km long, 55°NW-dipping seismic strip, along which a left-lateral slip took place. Using the Kanamori (1977) relation to derive a 1.8×10^{14} N m seismic moment from the 3.5 magnitude, and assuming a 30 GPa rigidity, we estimate the average slip on this 0.6 km^2 rupture surface to have been 1 cm.

Perhaps the most interesting point in Fig. 7 is the position of the three events that occurred in the decade preceding the mainshock (open circles): they are clearly out of the rupture plane and do not collapse into the N122°E-trending seismic alignment. The largest-magnitude event (largest open circle in Fig. 7) that occurred in 1997, 16 months before the mainshock, should not finally be called a foreshock. It is a remarkable result of Waldhauser's (2001) technique to leave these three events outside of the cluster. However, we note that the focus of the 1997 event lies close to the prolongation of the rupture plane to the NW, and also close to the Brion Fault. Therefore, this event, even if it cannot be called a foreshock, could have been produced by a left-lateral slip along that same fault, as its focal mechanism will support it (Section 6).

A final comment on Fig. 7 concerns the four late 'aftershocks' that could be relocated (black circles). One of them is abnormally deep (9.2 km); the three others are located in the upper fringe of the rupture surface. The epicentre of the largest-magnitude aftershock ($M_L = 2.4$) coincides with that of the mainshock; its focal depth is slightly shallower (2.4 versus 2.9 km). It is therefore legitimate to consider those three events as aftershocks, even though they occurred more than 1 year after the mainshock.

6 FAULT-PLANE SOLUTIONS

In this study, we used earthquakes with a minimum of eight polarity readings. We eventually kept fault-plane solutions when we judged them sufficiently constrained. Using the FPFIT software

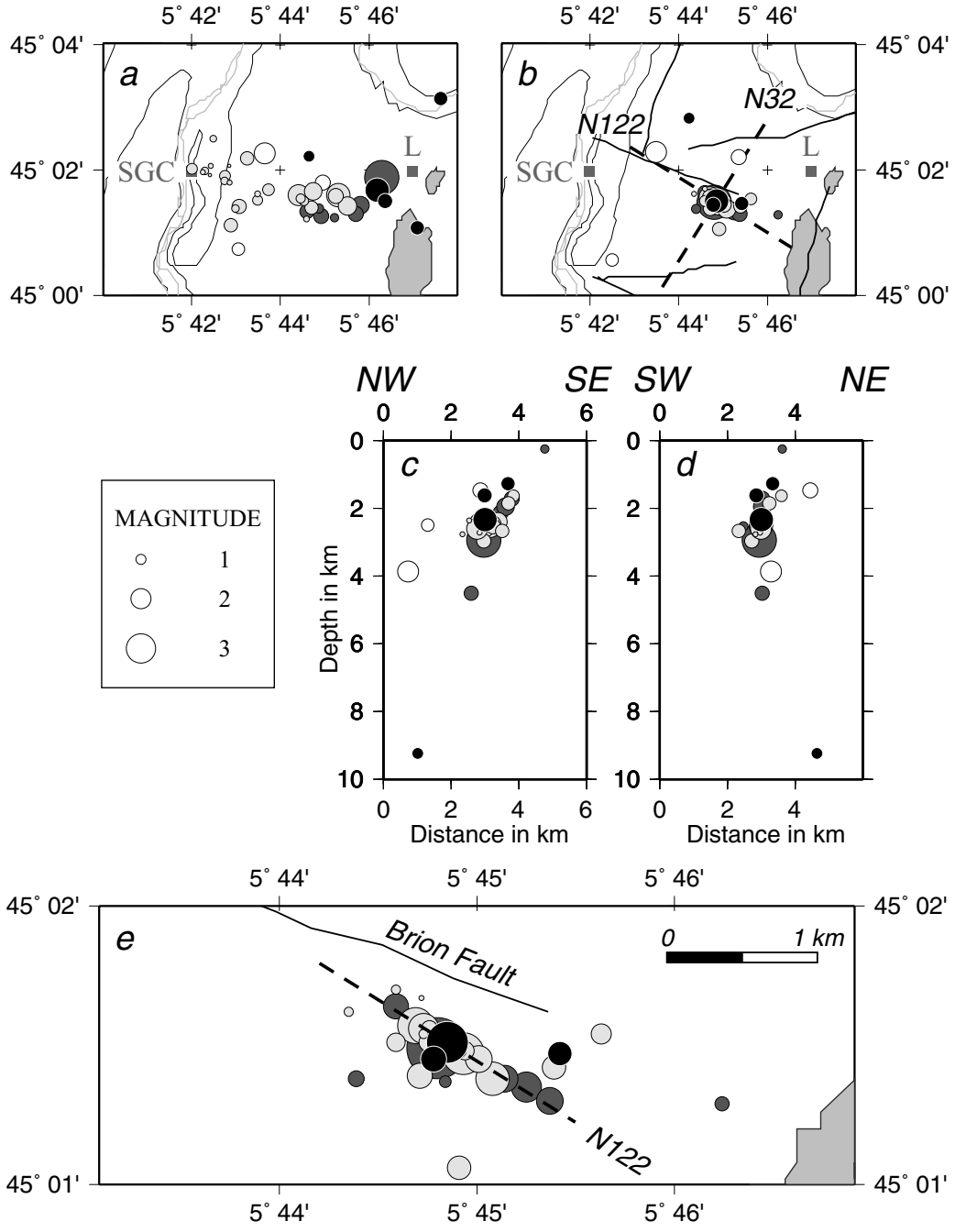

Figure 7. (a) Routine location of seismic events in the Laffrey area; open circles = three shocks before 1999 January 11; dark grey = mainshock and aftershocks before 1999 January 26; light grey = aftershocks after 1999 January 27; black = five late aftershocks (March–September 2000); (b) double-difference location (Waldhauser's technique (2001)), showing a collapse of most aftershocks into a N122°E-trending zone; only 80 per cent of the events could be relocated; (c) N122°E along-strike section; (d) N32°E cross-section; (e) close-up of the N122°E-trending aftershock zone. L = Laffrey; SGC = Saint-Georges-de-Commiers; maps include the hydrographic and geological features of Fig. 4.

(Reasenberg & Oppenheimer 1985), we obtained fault-plane solutions for 25 earthquakes in the 1.3–3.5 magnitude range (Fig. 8). Two of them (940204 and 940901) have double solutions, both very close. In Figs 5 and 8, the distribution of data points, either close to the circumference of the diagram or along concentric circles, results from the crude velocity model we used. However, as strike-slip mechanisms are preponderant, the consequences of this artefact on the robustness of the solutions do not give us much cause for concern.

Table 4 lists the 27 solutions plotted in Fig. 8. It also includes uncertainties on strike, dip and rake, as well as the station distribution ratio (STDR) for each solution. On average, strikes are better constrained (8°) than dips or rakes (20°), because most mechanisms are strike-slip mechanisms. STDR is a ratio between 0 and 1, which is

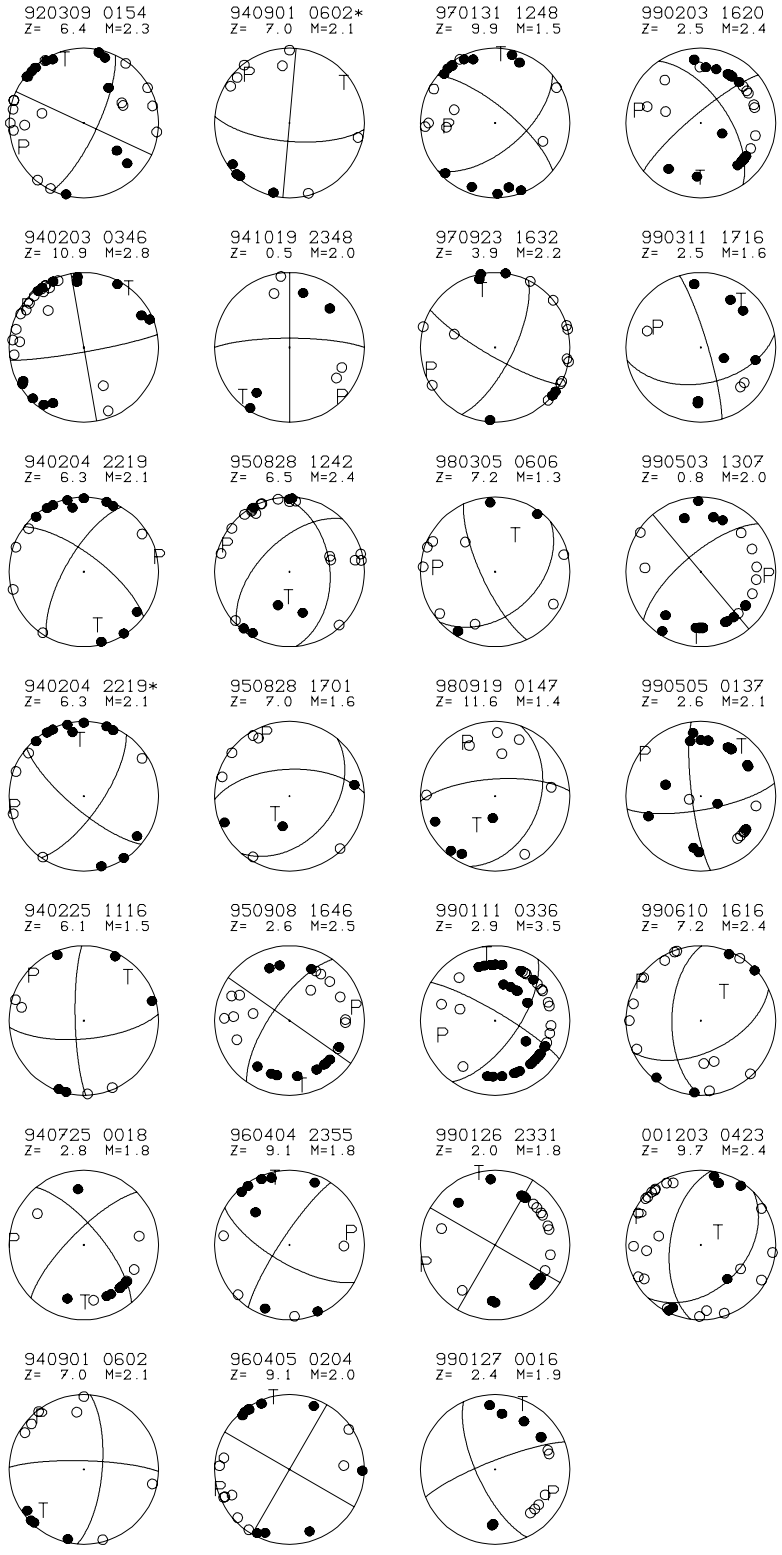

Figure 8. 27 detailed focal solutions for the 25 events discussed in the text. (See Table 4 for parameters.) The heading over each diagram reads date, origin time, depth and magnitude. The star indicates a double solution.

sensitive to the distribution of the data on the focal sphere (the higher the ratio, the more robust the solution). In Table 4, the mean STDR is 0.70, with extreme values of 0.52 and 0.82, which is quite satisfactory.

Fig. 9 shows the fault-plane solutions plotted on to the tectonic scheme of the study area. The fault-plane solutions for seven events of the Laffrey sequence were plotted along a direction perpendicular to the BBF, in order to better distinguish them from other events; we

Table 4. Parameters of the 27 focal solutions plotted in Fig. 8. p1, d1, and r1 are the dip direction, dip, and rake of the first nodal plane; p2, d2, and r2 of the second; pP and dP are the azimuth and plunge of the P axis; pT and dT of the T axis; Ds, Dd and Dr are uncertainties on the strike, dip and rake; STDR is the station distribution ratio. Two double solutions are identified by a star on the right.

Date	hh:mn:ss	Lat.	Long.	Depth	Mag	p1	d1	r1	p2	d2	r2	pP	dP	pT	dT	Ds	Dd	Dr	STDR
920309	01:54:34.35	45°09.3	5°52.6	6.4	2.3	115	75–180	25	90	−15	249	11	341	11	5	8	15		0.69
940203	03:46:00.75	45°37.4	5°41.1	10.9	2.8	170	85–180	80	90	−5	305	4	35	4	5	35	25		0.78
940204	22:19:46.65	45°23.4	6°04.2	6.3	2.1	300	70	160	37	71	21	78	1	169	28	5	25	30	0.68
940204	22:19:46.65	45°23.4	6°04.2	6.3	2.1	220	75	20	124	70	164	262	3	353	25	5	10	40	0.70*
940225	11:16:55.52	44°56.4	5°32.8	6.1	1.5	175	70	170	268	80	20	310	7	43	21	23	53	30	0.77
940725	00:18:57.01	45°10.7	5°53.0	2.8	1.8	315	75	160	50	70	16	273	3	182	25	5	18	20	0.64
940901	06:02:28.63	45°22.6	5°43.2	7.0	2.1	95	70	10	1	80	160	320	7	227	21	10	45	40	0.80
940901	06:02:28.63	45°22.6	5°43.2	7.0	2.1	185	70	180	275	90	20	318	14	52	14	8	20	10	0.75*
941019	23:48:33.97	45°23.2	5°43.1	0.5	2.0	90	90	10	360	80	180	135	7	225	7	8	25	40	0.76
950828	12:42:29.60	45°32.8	6°07.1	6.5	2.4	85	45	50	314	57	123	292	7	189	62	3	10	15	0.61
950828	17:01:08.01	45°33.0	6°07.6	7.0	1.6	130	40	50	357	60	118	338	11	225	63	20	28	15	0.75
950908	16:46:57.23	45°12.5	5°54.7	2.6	2.5	35	90	20	305	70	180	78	14	172	14	3	10	10	0.66
960404	23:55:23.44	45°14.3	5°57.2	9.1	1.8	210	70	−10	303	80–160	78	21	345	7	10	38	50		0.82
960405	02:04:05.83	45°15.2	5°57.4	9.1	2.0	30	90	0	300	90	180	255	0	345	0	10	45	40	0.82
970131	12:48:31.54	45°11.5	5°55.8	9.9	1.5	140	60–160	39	72	−32	266	34	2	8	8	30	40		0.78
970923	16:32:48.38	45°02.3	5°43.5	3.9	2.2	210	80	20	116	70	169	252	7	345	21	0	35	20	0.70
980305	06:06:45.37	44°57.6	5°41.6	7.2	1.3	245	75	50	137	42	157	274	20	25	45	10	10	5	0.63
980919	01:47:04.60	45°32.6	6°08.1	11.6	1.4	110	40	30	356	71	126	330	18	217	50	10	20	15	0.67
990111	03:36:36.35	45°01.5	5°44.8	2.9	3.5	125	65–170	30	80	−25	255	24	350	11	8	8	10		0.62
990126	23:31:41.72	45°01.4	5°45.2	2.0	1.8	30	90	0	300	90	180	255	0	345	0	5	25	30	0.65
990127	00:16:22.46	45°01.4	5°45.1	2.4	1.9	245	70	−10	338	80–160	113	21	20	7	18	35	50		0.74
990203	16:20:24.93	45°01.5	5°44.9	2.5	2.4	320	80	150	55	60	12	281	13	184	28	5	5	15	0.52
990311	17:16:08.20	45°01.4	5°45.0	2.5	1.6	170	50–170	73	82	−40	294	33	38	21	3	8	10		0.58
990503	13:07:51.10	45°24.3	5°44.2	0.8	2.0	50	90	20	320	70	180	93	14	187	14	10	28	35	0.77
990505	01:37:57.25	45°01.6	5°44.7	2.6	2.1	170	75	170	262	80	15	306	4	37	18	10	13	10	0.64
990610	16:16:10.79	45°32.2	6°08.2	7.2	2.4	155	55	140	270	58	42	302	2	35	51	10	18	20	0.70
001203	04:23:59.27	45°11.1	5°52.8	9.7	2.4	135	40	120	278	56	67	294	9	47	69	8	13	0	0.64

plotted them chronologically from left to right (970923 to 990505), although this does not necessarily correspond to a migration of epicentres from the NW to the SE (see the discussion in Section 7).

Along the BBF, between Vizille and Allevard, mechanisms are very consistent, with a predominant dextral strike-slip component along a N36°E ± 9°-striking plane. On average, the fault plane is vertical (90° ± 20°). One notable exception to this strike-slip series is the 001203 event, which has a clear reverse-faulting mechanism. Its nodal planes strike N8°E and N45°E. The second value is close to the mean direction computed above for the BBF (N36°E); the second nodal plane has a 40° dip to the SE, whereas the first has a steeper dip (56°) to the NW; tectonically, a reverse fault dipping to the SE is more plausible because the overthrust of the Belledonne massif on the Subalpine basement has long been postulated (Goguel 1943; Ménard 1979; Thouvenot & Perrier 1980; Guellec *et al.* 1990; Thouvenot & Ménard 1990). These three reasons make the N45°E-striking, 40°SE-dipping nodal plane the probable fault plane for this event.

Further to the NE, most earthquakes clustering along the Isère River in the Montmélian area have clear reverse-faulting mechanisms. Bearing in mind the possible overthrust of the Belledonne massif on the Subalpine basement mentioned above, our preferred fault plane will be that dipping to the SE. With this assumption, the fault-plane strike is ill-defined (N80°E ± 70°), while the mean dip is 45° ± 7° to the SE. The seismic activity of this area should not be viewed as directly related to that of the BBF. It should rather be considered a transition zone between two strike-slip faults, namely the BBF and what could be called the Subalpine Fault, a continuation of the BBF to the NE, beyond the study area, with a still unclear course.

The Laffrey sequence shows another peculiarity, which justifies the chronological plot of its focal solutions in Fig. 9. We first note that event 970923, the mainshock (event 990111) and event 990126 have almost identical strike-slip mechanisms. For event 990127, the focal solution shows nodal planes rotated clockwise by 35°, and subsequent mechanisms even amplify this rotation. Before January 26, and in accordance with the N122°E trend of the aftershock swarm, we can easily identify the mean fault plane as striking N120°E and dipping 90° ± 10°; after January 27, the identification of the fault plane from the focal mechanisms is unclear. If we choose the fault plane to obtain a left-lateral slip consistent with that observed for the beginning of the sequence, the mean strike is N159°E ± 12°, while the fault plane remains vertical (90° ± 20°). The complexity reflected in the unusually long duration of the aftershock sequence can also be observed in terms of migration along the fault plane. In Fig. 10, we plotted the sequence for the 140 d after the mainshock as a function of the position of epicentres along the N122°E direction. Early aftershocks (January 11–26) migrated to the east, while late aftershocks (January 27–May 5) concentrated closer to the mainshock.

The map of Fig. 9 also shows six mechanisms for isolated events. Most of them are strike-slip mechanisms; the *P* axes have a mean N120°E ± 20° azimuth. Table 5 summarizes fault-plane strikes and dips, and *P*-axis azimuths for the different seismic provinces.

7 DISCUSSION AND CONCLUSIONS

Revisiting the historical seismicity of the Grenoble region allowed us to demonstrate that, over the past two and a half centuries, the south of the study area along the Drac valley and the Belledonne border hills between Vizille and Theys have been the place of small

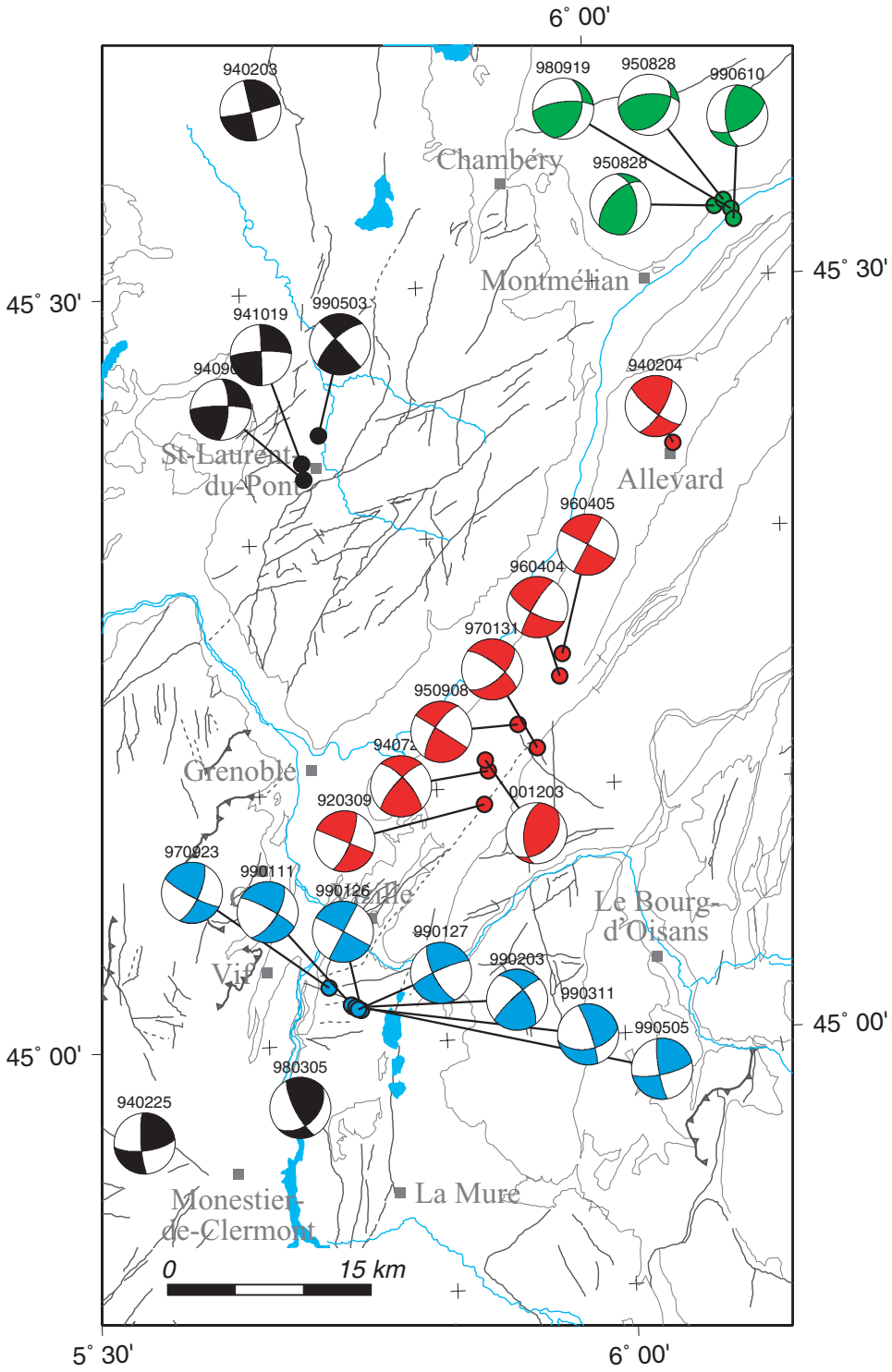

Figure 9. Seismotectonic provinces in the study area. Red, Belledonne Border Fault *stricto sensu* (mainly strike slip); green, Upper Isère valley (reverse faulting); blue, Laffrey (strike slip, with the solutions plotted chronologically along the preferred N122°E fault-plane strike); black, isolated events (strike slip). Geological background from Fig. 4.

to moderate earthquakes, up to MSK intensity VII. Our catalogue includes several new earthquakes that have never been properly investigated because they had been only faintly felt. However, it seems relevant to take these events into consideration because, paradoxically, their macroseismic epicentres can be better ascertained than those of major events. As a result of the low seismicity level, this is essential for identifying faults active in the past.

The same is true for instrumental seismicity. The Sismalp network allowed us to lower the detection level for earthquakes in the western Alps down to magnitude ∼1.3, which means that we can now locate

Table 5. Mean strikes and dips of the fault planes (when identified), and mean P-axis azimuths in the different seismic provinces discussed in the text. For the BBF *stricto sensu,* the reverse-faulting mechanism of event 001203 was not taken into account.

Province	Number of events	Strike (deg)	Dip (deg)	P-axis azimuth (deg)
Belledonne Border Fault s.s.	7	36 ± 9	90 ± 20	80 ± 8
Upper Isère valley	4	80 ± 70	45 ± 7 SE	140 ± 20
Laffrey (early sequence)	3	120	90 ± 10	74 ± 2
Laffrey (late sequence)	4	159 ± 12	90 ± 20	114 ± 10
Isolated events	6			120 ± 20

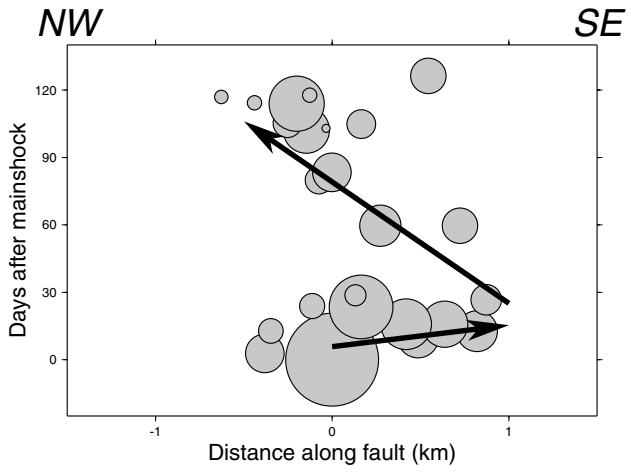

Figure 10. Migration of the Laffrey events along the N122°E direction (position of the mainshock = zero of the horizontal axis). Early aftershocks (January 11–26) show a migration to the SE, while late aftershocks (January 27–May 5) show a migration to the NW.

all $M_L > 1.3$ events, as well as a few $M_L < 1.3$ events. Without such a low detection level, we would not have been able to map a N30°E-trending, ∼50 km long seismic alignment between Monestier-de-Clermont and Allevard where most historical events have occurred. Although the term 'alignment' would be more correct, we call this seismic lineation the Belledonne Border Fault. The present data do not allow us to state whether it is a single fault or a fault zone.

In contrast to other faults in southeastern France—namely the Nîmes Fault and the Cévennes Fault—which have been postulated to be active on the grounds of geological or geomorphic information without any seismic activity being observed, the BBF is seismically active without any fault being mapped at the surface. In fact, a short segment of the BBF east of Vizille might coincide with the Vizille Fault (segment 4 of the Belledonne Middle Fault in Fig. 4); but the central and northeastern part of the BBF, deep-seated in the crystalline basement beneath the thick and densely wooded Mesozoic cover of the Belledonne massif, shows no relation with surface tectonics and the Belledonne Middle Fault. However, our conclusion, that the BBF for the most part has no corresponding surface expression, might evolve in the future when existing geological data are reappraised, and new tectonic observations gathered in the field.

On another side, geomorphic features should not be misused. Fig. 11 shows for instance a detail of the topography along the central part of the BBF. Two steep increases can be observed: (1) where the border hills of the Belledonne massif rise over the Isère valley and (2) where the *Rameau interne* of the Belledonne massif rises towards its maximal height. Between these two steep slopes, the seismicity is coincident with a somewhat flatter topography which corresponds to the Aalenian argillite monocline of the *Balcon de Belledonne* (shown by two arrows). This should be considered a mere coincidence, since seismic events are deep-seated in the crystalline basement, at a mean 7 km depth.

All but one of the focal solutions along the BBF are strike-slip mechanisms, with a vertical fault plane striking N36°E and a right-lateral movement. This is consistent with the anticlockwise rotation of the Adriatic indenter about a pole located in the Po plain (Anderson & Jackson 1987), or with the anticlockwise rotation of the Mont-Blanc–Belledonne–Pelvoux massifs speculated by Ménard (1988) or Vialon *et al.* (1989). It also seems to be consistent with the analysis of geodetic data for the 1946–1999 period in which Martinod *et al.* (1996, 2001) derived a differential movement between Chartreuse and Belledonne consistent with a right-lateral strike-slip along the Isère valley at a rate of ∼5 mm yr^{-1}. This value is very large for the western Alps, since permanent GPS data show that the relative speed of the Adriatic plate with respect to stable Europe is smaller than 5 mm yr^{-1} (Calais 1999). Creep should therefore take place along the BBF, and this phenomenon should be much more important than the millimetric slip yielded by sporadic small-magnitude earthquakes. However, these geodetic results obviously need several more years of observation to be fully ascertained. The Observatoire de Grenoble is currently installing two new permanent GPS sites in the Chartreuse and Belledonne massifs, with the hope of shortening the observation period necessary to obtain reliable results.

The southwestern tip of the BBF terminates south of Vizille, where the 1999 $M_L = 3.5$ Laffrey earthquake occurred. By relocating the many aftershocks that followed this moderate-magnitude shock, we demonstrate that the aftershock zone trends N122°E, a direction perpendicular to that of the BBF. Although this conjugate fault (Brion Fault) has been mapped before the earthquake occurred, its importance has never been recognized and its role has never been ascertained. The focal mechanism of the mainshock and those of two other events establish its left-lateral strike-slip. Fig. 12 shows that the Brion Fault probably extends to the W–NW through a small defile across a calcareous range SE of Vif. The Brion Fault could also explain other topographic features on the western flank of the Vercors massif, where it could possibly join a reverse fault.

The geometry of the rupture is peculiar: it is confined to a narrow, 55°NW-dipping strip, in the 1.6–3.0 km depth range (crystalline basement). From the position of the mainshock at the bottom of this strip, one can imagine that the rupture initiated there, then propagated crosswise upwards, while the left-lateral slip kept horizontal. Such a dipping rupture strip seems unusual for a strike-slip mechanism. For instance, along the Hayward strike-slip fault, California, Waldhauser *et al.* (1999) described *horizontal* alignments of hypocentres (hence parallel to the slip direction), and interpreted them as streaks outlining zones where brittle failure conditions were met. In our case, although the focal mechanism shows pure strike-slip, we do not recognize this kind of geometry.

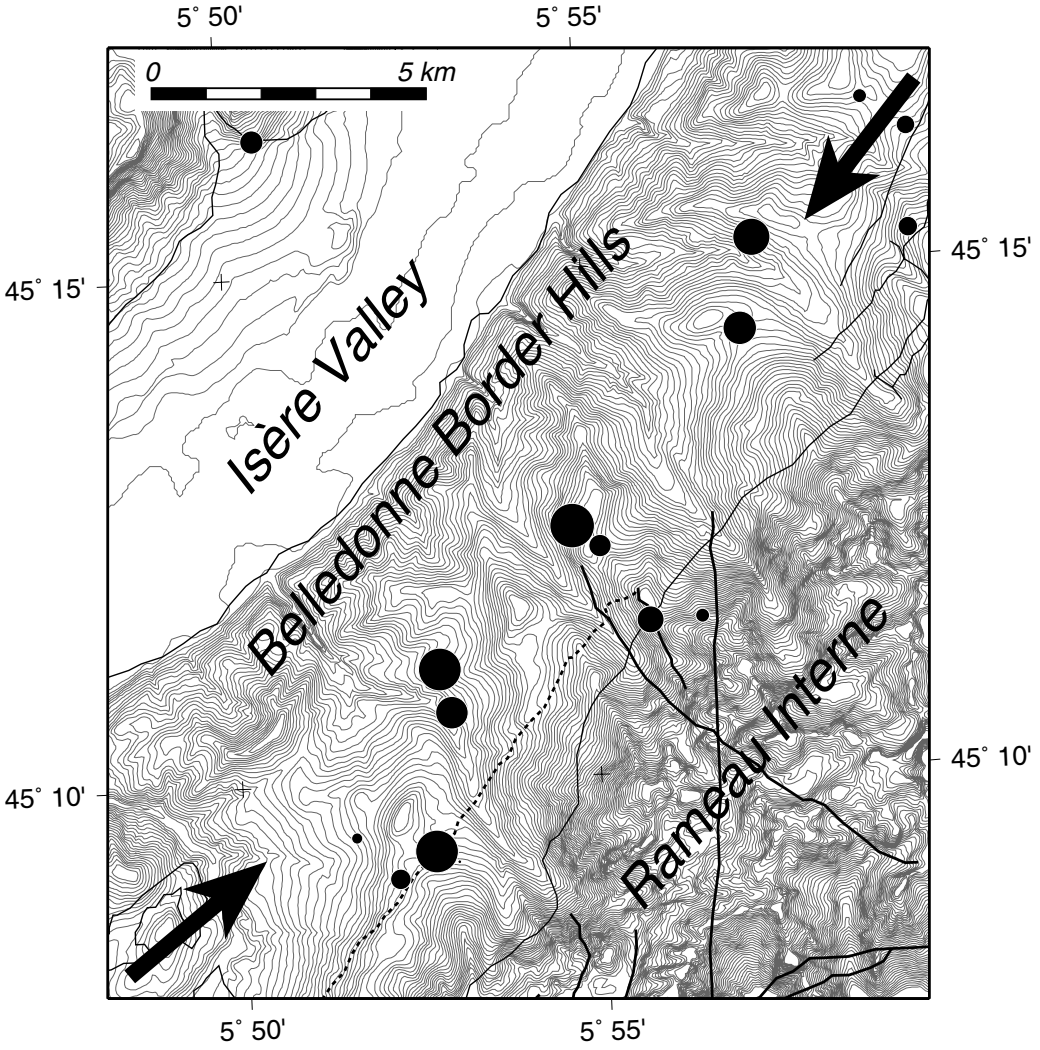

Figure 11. Close-up on the topography along the central part of the BBF. Contours at 25 m vertical interval. The seismicity is coincident with a somewhat flatter topography of the border hills which corresponds to the Aalenian argillite monocline of the *Balcon de Belledonne* (shown by two arrows).

One can wonder why the Laffrey earthquake ruptured the Brion Fault, and not the BBF. Alternatively, one could even postulate that it ruptured the BBF, but triggered activity on the otherwise-locked Brion Fault. Given the almost pure strike-slip mechanism of the mainshock, with two nodal planes striking at right angles, and given the location of the mainshock epicentre at the place where the BBF meets the Brion Fault, we cannot completely exclude this hypothesis. By stating that the Laffrey earthquake and its aftershock sequence originated on the Brion Fault, we merely chose the simplest explanation. The same is true for the BBF itself, which could be seen as the juxtaposition, in a N30°E direction, of earthquakes occurring on N120°E-striking left-lateral faults. However, the slashing of the basement by so many faults, with epicentres happening to line up along a perpendicular direction, makes the hypothesis unlikely. Again, it is simpler here to postulate a N30°-striking right-lateral fault (or fault zone).

We postulate that the Brion Fault offsets the BBF by ∼5 km to the west, since historical seismicity (Fig. 3b) as well as instrumental seismicity (Fig. 3a) show seismic activity in a N–S direction along the Drac river. We believe that the 1963 $M_L = 4.9$ Monteynard earthquake, which is thought to have been triggered by the filling of the 127 m high, 2.76×10^8 m^3 Monteynard reservoir (e.g. Grasso *et al.* 1992), was located at the confused southwestern tip of the BBF (Fig. 12). This is a matter of concern, even if the concrete vault dam performed well and suffered no damage in 1963. The 1962 $M_L = 5.3$ Corrençon earthquake, located deep within the Vercors massif (Fig. 3b), seems to have resulted from the slip of a N150°E-striking fault that abuts on the southern continuation of the BBF in the Monteynard area. At the opposite end, NE of Allevard, the course of the BBF is ill-defined. The seismicity observed in the Upper Isère Valley clearly involves reverse-faulting mechanisms.

No catastrophic event has ever been reported over the last centuries along the BBF. Its length of ∼50 km leaves enough space for a magnitude 7 event to take place. Hence, the magnitude value of 6.5 that is usually considered a maximum for an earthquake in the Grenoble area may underestimate the reality. With only a few tens of earthquakes along the BBF over the last 12 yr, a Gutenberg–Richter statistical analysis would be meaningless. Statistics gathered by the Sismalp network over the last 12 yr for more than 6000 earthquakes in southeastern France yield a *b*-value very close to 1 and a mean recurrence interval of 300 yr for magnitude 6 events. By simply taking into account the 3:100 ratio between the seismic activity in the

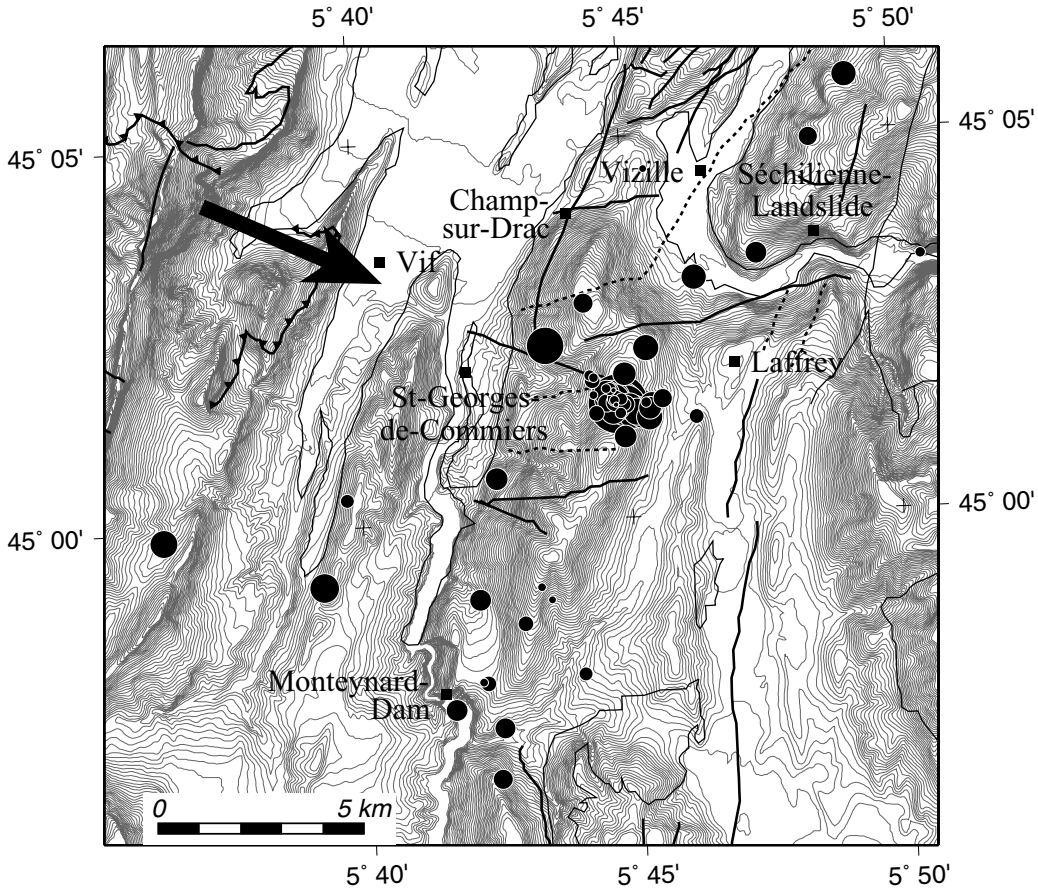

Figure 12. Close-up on the topography along the southwestern end of the BBF. Contours at 25 m vertical interval. The Brion Fault, responsible for the Laffrey earthquake and its aftershock sequence, probably extends to the NW through a small defile across a calcareous range SE of Vif (arrow).

study area and that in southeastern France, we find that the mean recurrence interval for magnitude 6 events along the BBF is 10000 yr. If we apply to the BBF the same power law as for southeastern France ($b = 1$), aseismic segments observed along the BBF, if they reveal themselves as seismic gaps (Fig. 3a), would leave enough space for magnitude 5 events, with recurrence intervals of 1000 yr. With what is now known about site effects in the up to 500 m thick unlithified Quaternary deposits of the Isère Valley, which can amplify the ground motion by a factor of 10 (Le Brun *et al.* 2001), such an occurrence could cause extensive damage. An example is provided by the macroseismic maps for the 1962 $M_L = 5.3$ Corrençon earthquake (Rothé 1972; Levret *et al.* 1996). Isoseismal V (which delimits the area where damage was observed) extends much further (up to 40 km) in the N45°W–N135°E azimuthal sector (Isère and Drac valleys) than towards the inner part of the Vercors massif to the SW (10 km). For this earthquake, isoseismals in the Grésivaudan also show clear twists to the NE produced by site effects. Another topic of concern is that the southwestern part of the BBF is very close to the Séchilienne landslide (Fig. 12), an unstable volume of $2–10 \times 10^7$ m^3 over a 45° mean slope. When assessing the risk, one should now take into account that the landslide could be triggered by an earthquake only 1 km away.

Regarding Alpine tectonics, the activity of the BBF and its right-lateral strike-slip characteristics stress the importance of the N30°E–N40°E direction in the present-day tectonics of the western Alps. This legacy of the Variscan orogenesis can no longer be ignored, and will now have to be taken into account in future geodynamic models of the Alpine edifice. The rare seismic events we located along the northwestern border of the Chartreuse massif and further north are clues that the differential movement between stable Europe and the Adriatic indenter extends much further west and north into the passive European margin. In decades to come, other seismic alignments—more external to the BBF—might be discovered in this outer part of the western Alps.

ACKNOWLEDGMENTS

The presence of Robert Guiguet has been of paramount importance for installing and servicing the Sismalp network over the past 15 yr. The Conseil général de l'Isère, the Délégation aux risques majeurs (French Ministry of the Environment), the Institut national des sciences de l'Univers (CNRS), the Conseil régional Rhône-Alpes and the Pôle grenoblois des risques naturels funded the Sismalp network. The Bureau central sismologique français, the Observatoire de Grenoble, and several County Councils (Isère, Alpes-de-Haute-Provence, Haute-Savoie, Ain, Drôme and Savoie) support its running costs. We are indebted to the many officials in these funding agencies who realized that earthquake monitoring can be a long and exacting labour, and who have trusted us for so many years. Data from other seismic networks (RéNaSS, LDG, SED and IGG) were used when available. Along the BBF and in the Laffrey epicentral

area, temporary stations could be kept in service for several months, thanks to the willingness of Messrs and Mrs Bouchon, Chillon, Dorel, Fraile and Ravanat. Jérémie Ferrand helped to process the data elevation model. Jacques Dorel read a first version of this article and suggested improvements; Ron Wilkins checked the final version. Figures were drawn by using the GMT software (Wessel & Smith 1998). This is EOST contribution no 2003.12-UMR7516.

REFERENCES

Allard, G., *ca.*, 1710. La description historique de la ville de Grenoble, p. 310, in *Bibliothèque Historique et Littéraire du Dauphiné,* Vol. 1, pp. 239–338, ed. Gariel, H., 1864.

Anderson, H. & Jackson, J., 1987. Active tectonics in the Adriatic region, *Geophys. J. R. astr. Soc.,* **91,** 937–983.

Barféty, J.-C. & Gidon, M., 1996. La structure des Collines bordières du Grésivaudan et des secteurs adjacents, à l'est de Grenoble (Isère, France) (cartes géologiques à 1/50 000 Domène et Vizille), *Géol. Alpine,* **72,** 5–22.

Barféty, J.-C., Menot, R.-P., Gidon, M. & Debon, F., with the collaboration of Pêcher, A., Guillot, S., Fourneaux, J.-C., Gamond, J.-F. & Mouterde, R., 2000. *Notice Explicative, Carte géol. France (1/50 000), Feuille Domène (773),* BRGM, Orléans, p. 187, Geological map by J.-C. Barféty *et al.* (2001).

Bureau Central Sismologique Français, 2002. Sismicité de la France en 1997, 1998 et 1999, *Observ. Sismol.,* **1,** 95.

Calais, E., 1999. Continuous GPS measurements across the western Alps, 1996–1998, *Geophys. J. Int.,* **38,** 221–230.

Chorier, N., 1672. *Histoire Gén. Dauphiné,* **1,** 372.

Deichmann, N., 1992. Structural and rheological implications of lower-crustal earthquakes below northern Switzerland, *Phys. Earth planet. Inter.,* **69,** 270–280.

Deville, É. & Chauvière, A., 2000. Thrust tectonics at the front of the western Alps: constraints provided by the processing of seismic reflection data along the Chambéry transect, *C.R. Acad. Sci. Paris,* **331,** 725–732.

Fréchet, J., 1978. Sismicité du Sud-Est de la France et une nouvelle méthode de zonage sismique, *Thesis,* Université de Grenoble, France.

Fréchet, J. & Thouvenot, F., 2000. Pickev 2000, ftp://sismalp.obs.ujf-grenoble.fr.

Gidon, M., 1998–2002. GEOL-ALPES, http://www.geol-alpes.com.

Goguel, J., 1943. *Introduction à l'Étude Mécanique des Déformations de l'Écorce Terrestre,* p. 514, Nation., Paris.

Grasso, J.-R., Guyoton, F., Fréchet, J. & Gamond, J.-F., 1992. Triggered earthquakes as stress gauge: implication for the upper-crust behaviour in the Grenoble area, *Pageophys.,* **139,** 579–605.

Grellet, B., Combes, P., Granier, T., Philip, H. & Mohammadioun, B., 1993. Sismotectonique de la France métropolitaine dans son cadre géologique et géophysique avec atlas de 23 cartes au 1/4 000 000 et une carte au 1/1 000 000, *Mém. Soc. géol. France,* **164,** 76.

Guellec, S., Mugnier, J.-L., Tardy, M. & Roure, F., 1990. Neogene evolution of the western Alpine foreland in the light of ECORS data and balanced cross-section, *Mém. Soc. géol. France,* **156,** 165–184.

Kanamori, H., 1977. The energy release in great earthquakes, *J. geophys. Res.,* **82,** 2981–2987.

Lacassin, R., Meyer, B., Benedetti, L., Armijo, R. & Tapponnier, P., 1998. Geomorphic evidence for Quaternary sinistral slip on the Cévennes Fault (Languedoc, France), *C.R. Acad. Sci. Paris,* **326,** 807–815.

Lambert, J. & Levret-Albaret, A. (eds), 1996. *Mille ans de Séismes en France, Catalogue d'Épicentres Paramètres et Références,* p. 80, Ouest Editions, Presses académiques.

Lambert, J., ed., 1997. *Les Tremblements de Terre en France,* p. 196, Editions BRGM.

Le Brun, B., Hatzfeld, D. & Bard, P.-Y., 2001. Site effect study in urban area: experimental results in Grenoble (France), *Pageophys.,* **158,** 2543–2557.

Lee, W.H.K. & Lahr, J.C., 1975. HYPO71 (revised): a computer program for determining hypocenter, magnitude, and first motion pattern of local earthquakes, *US Geol. Surv. Open-File Report*, 75–311, 110.

Lemoine, M., de Graciansky, P.C. & Tricart, P., 2000. *De l'Océan à la Chaîne de Montagnes: Tectonique des Plaques dans les Alpes,* p. 207, Gordon & Breach, Paris.

Levret, A., Cushing, M. & Peyridieu, G., 1996. *Recherche des Caractéristiques de Séismes Historiques en France. Atlas de 140 Cartes Macrosismiques* (2 vols), p. 399, Institut de Protection et de Sûreté Nucléaire.

Martinod, J., Jouanne, F., Taverna, J., Ménard, G., Gamond, J.-F., Darmendrail, X., Notter, J.-C. & Basile, C., 1996. Present-day deformation of the Dauphiné Alpine and Subalpine massifs (SE France), *Geophys. J. Int.,* **127,** 189–200.

Martinod, J., Roux, L., Gamond, J.-F. & Glot, J.-P., 2001. Déformation actuelle de la chaîne de Belledonne (Massifs cristallins externes alpins, France): comparaison triangulation historique–GPS, *Bull. Soc. géol. Fr.,* **172,** 713–722.

Ménard, G., 1979. Relations entre structures profondes et structures superficielles dans le Sud-Est de la France. Essai d'utilisation de données géophysiques, Thèse, Université de Grenoble.

Ménard, G., 1988. Structure et cinématique d'une chaîne de collision. Les Alpes occidentales et centrales, *Thèse d'État*, Université de Grenoble.

Montessus de Ballore, F. de, 1905. *Notes sur l'Histoire des Séismes dans le Monde Entier, des Origines à 1905,* Manuscript, Société de Géographie, Dépôt Bibliothèque Nationale de France, Paris.

Paul, A., Cattaneo, M., Thouvenot, F., Spallarossa, D., Béthoux, N. & Fréchet, J., 2001. A three-dimensional crustal velocity model of the south-western Alps from local earthquake tomography, *J. geophys. Res.,* **106,** 19 367–13 389.

Reasenberg, P.A. & Oppenheimer, D., 1985. FPFIT, FPPLOT and FPPAGE: Fortran computer programs for calculating and displaying earthquake fault-plane solutions, *US Geol. Surv. Open-File Report,* 85–739, 109.

Rothé, J.-P., 1941. Les séismes des Alpes françaises en 1938 et la séismicité des Alpes occidentales, *Ann. Inst. Phys. Globe Strasbourg,* **3,** 1–105.

Rothé, J.-P., 1972. La séismicité de la France de 1961 à 1970, *Ann. Inst. Phys. Globe Strasbourg,* **9,** 3–134.

Scholz, C.H., 1990. *The Mechanics of Earthquakes and Faulting,* p. 439, Cambridge University Press, Cambridge.

Sellami, S., Kissling, E., Thouvenot, F. & Fréchet, J., 1995. Initial reference velocity model for seismic tomography in the western Alps. (Poster) 20th Gen. Assembly of the European Geophysical Society, Hamburg.

SisFrance, 2002. http://www.sisfrance.net.

Solarino, S., Kissling, E., Sellami, S., Smriglio, G., Thouvenot, F., Granet, M., Bonjer, K.P. & Sleijko, D., 1997. Compilation of a recent seismicity database of the greater Alpine region from several seismological networks and preliminary 3D tomographic results, *Ann. Geofis.,* **XL,** 161–174.

Sue, C., 1998. Dynamique actuelle et récente des Alpes occidentales internes—approche structurale et sismologique, *Thesis,* Université de Grenoble.

Sue, C., Thouvenot, F., Fréchet, J. & Tricart, P., 1999. Widespread extension in the core of the western Alps revealed by earthquake analysis, *J. geophys. Res.,* **104,** 25 611–25 622.

Tapponnier, P., 1977. Évolution tectonique du système alpin en Méditerranée: poinçonnement et écrasement rigide–plastique, *Bull. Soc. géol. Fr.,* **7,** 437–460.

Thouvenot, F., 1981. Modélisation bidimensionnelle de la croûte terrestre en vitesse et atténuation des ondes sismiques. Implications géodynamiques pour les Alpes occidentales, *Thesis,* Université de Grenoble, France.

Thouvenot, F., 1996. Aspects géophysiques et structuraux des Alpes occidentales et de trois autres orogènes (Atlas, Pyrénées, Oural), *Thèse d'État,* Université de Grenoble.

Thouvenot, F. & Ménard, G., 1990. Allochthony of the Chartreuse Subalpine massif: explosion-seismology constraints, *J. Struct. Geol.,* **12,** 113–121.

Thouvenot, F. & Perrier, G., 1980. Seismic evidence of a crustal overthrust in the western Alps, *Pure appl. Geophys.,* **119,** 163–184.

Thouvenot, F., Fréchet, J., Guyoton, F., Guiguet, R. & Jenatton, L., 1990. SISMALP: an automatic phone interrogated seismic network for the western Alps, *Cah. Centr. Eur. Géodyn. Seismol.,* **1,** 1–10.

Thouvenot, F. *et al.*, 1998. The M_L 5.3 Épagny (French Alps) earthquake of 1996 July 15: a long-awaited event on the Vuache Fault, *Geophys. J. Int.,* **135,** 876–892.

Vialon, P., Ménard, G. & Rochette, P., 1989. Indentation and rotation in the western Alpine arc, *Spec. Publs geol. Soc. Lond.*, **45,** 329–338.

Villard, M., 1887. Météorologie régionale, *Bull. Soc. arch. Drôme,* **21,** 46–61.

Vogt, J., ed., 1979. *Les Tremblements de Terre en France,* p. 220, Éditions BRGM, Paris.

Waldhauser, F., 2001. hypoDD—a program to compute double-difference hypocenter locations, *US Geol. Surv. Open-File Report,* 01–113, p. 25.

Waldhauser, F. & Ellsworth, W.L., 2000. A double-difference earthquake location algorithm: method and application to the northern Hayward fault, California, *Bull. seism. Soc. Am.,* **90,** 1353–1370.

Waldhauser, F., Ellsworth, W.L. & Cole, A., 1999. Slip-parallel seismic lineations on the northern Hayward Fault, California, *Geophys. Res. Lett.,* **26,** 3525–3528.

Wessel, P. & Smith, W.H.F., 1998. New, improved version of Generic Mapping Tools released, *EOS, Trans. Am. geophys. Un.,* **79,** 579.